Novel analogs of antitumor agent calixarene 0118

European Journal of Medicinal Chemistry 89 (2015) 279–295

Contents lists available at ScienceDirect

European Journal of Medicinal Chemistry

journal homepage: http://www.elsevier.com/locate/ejmech

Original article

Novel analogs of antitumor agent calixarene 0118: Synthesis, cytotoxicity, click labeling with 2-[^{18}F]fluoroethylazide, and *in vivo* evaluation

Tilman Läppchen [a, *], Ruud P.M. Dings [b, c], Raffaella Rossin [a], Justine F. Simon [a], Ton J. Visser [d], Martine Bakker [a], Priya Walhe [a], Tiemen van Mourik [a], Katia Donato [a], Judy R. van Beijnum [e], Arjan W. Griffioen [e], Johan Lub [a, *], Marc S. Robillard [a], Kevin H. Mayo [b], Holger Grüll [a]

[a] Department Minimally Invasive Healthcare, Philips Research, High Tech Campus 11, 5656 AE Eindhoven, The Netherlands
[b] Department of Biochemistry, Molecular Biology & Biophysics, University of Minnesota Health Sciences Center, 6-155 Jackson Hall, 321 Church Street, Minneapolis, MN 55455, USA
[c] Department of Radiation Oncology, Winthrop P. Rockefeller Cancer Institute, University of Arkansas for Medical Sciences, 4301 W. Markham St., Slot 771, Little Rock, AR 72205-7199, USA
[d] Syncom BV, Kadijk 3, 9747 AT Groningen, The Netherlands
[e] Angiogenesis Laboratory, Department of Medical Oncology, VU University Medical Center, De Boelelaan 1118, 1081 HV Amsterdam, The Netherlands

ARTICLE INFO

Article history:
Received 13 September 2014
Received in revised form
15 October 2014
Accepted 16 October 2014
Available online 18 October 2014

Keywords:
Compound 0118
Calixarene
PET imaging
Click chemistry
Fluorine-18
Anti-angiogenic therapy

ABSTRACT

Calixarene 0118 is a potent anti-angiogenic agent that effectively inhibited tumor growth in preclinical studies, and is currently being evaluated in a phase I clinical trial. We have designed two close mimetics of calixarene 0118 containing a terminal alkynyl-functional group, and developed an optimized semi-automated procedure for radiolabeling with 2-[^{18}F]fluoroethylazide using click chemistry. Following semi-preparative HPLC purification and formulation, the lower-rim modified analog [^{18}F]**6** and the equatorially labeled [^{18}F]**13** were obtained in >97% radiochemical purity and overall decay-corrected isolated radiochemical yields of 18.7 ± 2.7% (n = 4) and 10.2 ± 5.0% (n = 4), respectively, in a total synthesis time of about 2 h. Preliminary *in vivo* studies in nude mice bearing human tumor xenografts revealed highest accumulation of both tracers in the liver, followed by spleen, kidney, lung and bone, with no substantial uptake in the tumor. Still, these first-in-class radiotracers are a valuable tool for pharmacokinetic profiling and improvement of calixarene-based anti-angiogenic therapeutics in the future, as similar radiolabeling strategies may be applied to other compounds in the calixarene series. The cold reference compounds of the radiotracers were characterized in terms of cytotoxicity and anti-proliferative effects on HUVEC cells and on MA148 human ovarian carcinoma cells, along with the respective precursors, a small series of 0118 analogs modified with short-chain linear alkyl substituents, and a PEG_3-spaced calixarene dimer. While all of the new analogs proved at least equipotent to parent 0118, some of them inhibited HUVEC and MA148 cell growth almost 4- and 10-fold more effectively, rendering these analogs promising candidates for further evaluation in anti-angiogenic cancer therapy.

1. Introduction

In the past decades, drug-based cancer therapy has evolved from general cytotoxic chemotherapy to increasingly complex personalized treatment regimens using drugs matching the specific targets of a particular cancer. Beside new generations of anti-proliferative cytotoxic drugs and anti-hormone therapies, an increasing number of anti-angiogenic agents – small molecules, peptides and therapeutic antibodies – have been developed and

Abbreviations: *n*-BuLi, *n*-butyl lithium; DMF, *N,N*-dimethylformamide; DMSO, dimethyl sulfoxide; HSQC, heteronuclear single quantum coherence; HUVEC, human umbilical vein endothelial cells; %ID/g, percentage of injected dose per gram of tissue; KO*t*Bu, potassium *tert*-butoxide; NaOMe, sodium methoxide; PBS, phosphate buffered saline; PEG, polyethylene glycol; PET-CT, positron emission tomography – computed tomography; SAR, structure–activity relationship; TFA, trifluoroacetic acid; VOI, volume of interest.

* Corresponding authors.
E-mail addresses: tilman.lappchen@philips.com, tilman1973@hotmail.com (T. Läppchen), johan.lub@philips.com (J. Lub).

http://dx.doi.org/10.1016/j.ejmech.2014.10.048
0223-5234/

many of those have progressed to the clinic [1]. Angiogenesis, the formation of new blood vessels from pre-existing vasculature, is a crucial prerequisite for primary tumor growth above a size of about 1–2 mm^3, and has also been found essential for development of metastases [2–4].

In the early years, most anti-angiogenic agents discovered were endogenous proteins that inhibit EC growth, e.g. platelet factor-4 (PF4), plasmin fragment angiostatin, collagen XVIII fragment endostatin, and bactericidal-permeability-increasing protein (BPI). Containing numerous hydrophobic and cationic residues, and a common antiparallel β-sheet motif, these proteins are characterized by a high level of compositional and structural similarity [5]. Based on these findings, a new generation of synthetic β-sheet forming peptide 33-mers have been designed, one of which, named anginex, showed particular potent anti-angiogenic activity *in vitro* and *in vivo* [6]. Anginex was found to inhibit tumor growth and reduce microvessel density both in murine melanoma and breast sarcoma models, and in athymic mice bearing different types of human tumor xenografts, among others LS174T colon adenocarcinoma, and MA148 and SKOV-3 ovarian carcinoma [7–10]. Extensive structure–activity studies established five hydrophobic residues in β-strands 1 and 2 on the same face of the amphipathic anti-parallel β-sheet structure of anginex as being essential for anti-proliferative activity, and formed the foundation for the design of a series of partial peptide mimetics containing a β-sheet-inducing dibenzofuran (DBF) turn, some of which more effectively inhibited tumor growth in mice than anginex [11].

Although anginex and its partial peptide mimetic 6DBF7 have shown promising anti-tumor effects *in vivo*, non-peptidic compounds are generally known to be superior drugs, mainly because they potentially allow oral administration, typically lack an immune response, and can be optimized in terms of chemical and metabolic stability, resulting in a better pharmacokinetic profile. With the overall backbone dimensions of key residues in the two-stranded beta-sheet of anginex roughly matching those of the calix[4]arene scaffold, calix[4]arene derivatives containing basic and hydrophobic substituents on the upper and lower rim, respectively, were envisioned as potential non-peptidic analogs of anginex. Indeed, from a library of 23 substituted calix[4]arene analogs, two candidates, termed compound 0118 and 1097, proved to be potent inhibitors of angiogenesis *in vitro*, and were found to reduce tumor growth and microvessel density in B16 murine melanoma and MA148 xenografts in athymic mice [12]. While since its discovery, calixarene 0118 (Fig. 1) was known to display multimodal activities similar to anginex, such as inhibition of endothelial cell proliferation, migration, and induction of apoptosis [12], it was only recently that both calixarene 0118 [13] and anginex [14] were discovered to also target the same receptor, galectin-1 (gal-1). Interestingly, SAR-data from anginex and HSQC mapping studies with calixarene 0118 indicate that both ligands interact with gal-1 via their hydrophobic surfaces [11,13]. This is very different from the majority of galectin-1 antagonists presently available, which are β-galactoside analogs and glycomimetics targeting the canonical β-galactoside carbohydrate binding site [15–17]. In fact, calixarene 0118 was established to act as a noncompetitive, allosteric inhibitor of gal-1, with its binding site being located at the back face of gal-1 opposite to the β-galactoside binding site [13]. In the meantime, after successful completion of extensive preclinical studies [12,18], calixarene 0118 (also known as PTX008, OTX008) is currently being evaluated by OncoEthix in a phase I clinical trial in patients with malignant advanced solid tumors (ClinicalTrials.gov: NCT01724320) [17], and ongoing early discovery research has led to the identification of an even more potent analog, PTX013 [19].

Despite the promising *in vitro* and *in vivo* data collected for lead compound 0118 and others in the series, radiolabeled analogs have not been reported so far, although they may prove highly valuable, both as a research tool and companion diagnostic to study target engagement *in vivo*, and for pharmacokinetic profiling of this class of compounds. Designing radiolabeled 0118 analogs without introduction of major structural changes is an intrinsically difficult task, particularly in view of the stringent structural constraints established in previous SAR-studies [12,13] indicating that only minor modifications are tolerated at the hydrophobic upper rim of the calixarene, and the symmetric nature of the lower rim substituents, which is introduced already at a very early stage in the previously reported chemical syntheses of these compounds. We

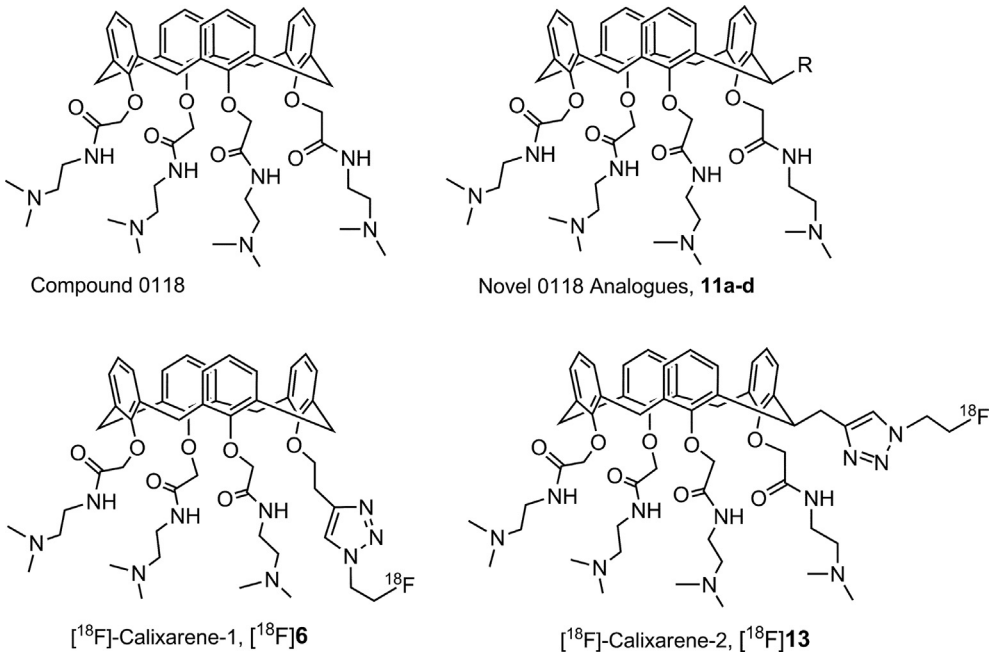

Fig. 1. Chemical structure of compound 0118, novel 0118 analogs **11a**–**d**, and radiotracers [^{18}F]**6** and [^{18}F]**13**.

have addressed these challenges by devising two alternative click chemistry based approaches building on the design of non-symmetrical 0118 analogs containing a terminal alkynyl functional group, either as an equatorial substituent at a methylene bridge position or as a replacement of one of the four lower rim substituents. Copper-catalyzed azide-alkyne cycloaddition (CuAAC) employing the well-established 2-[^{18}F]fluoroethylazide synthon then gave access to the corresponding radiolabeled triazole analogs, which structurally closely resemble the parent calixarene 0118 (Fig. 1).

Here, we report on the radiosynthesis of F-18 labeled calixarene 0118 analogs, including extensive optimization of CuAAC reaction conditions for this type of compounds, and the chemical synthesis of the precursors and reference compounds. In addition, we employed our alkynyl-precursors to prepare a 0118 dimer interconnected by a PEG_3-chain, and created a series of 0118 derivatives monosubstituted at an equatorial methylene bridge position with alkyl substituents of different chain length (Fig. 1). All compounds were characterized in terms of anti-proliferative activity *in vitro*, and the study was complemented by a preliminary *in vivo* investigation of both radiotracers in tumor-bearing mice.

2. Results and discussion

2.1. Chemistry

2.1.1. Synthesis of compound 0118 analogs with modified lower-rim substituents

Compared to compound 0118, synthesis of unsymmetrically substituted analogs is far more challenging, and a number of alternative routes towards click precursor **4** have been explored. The first pathway towards key intermediate **3** involves direct condensation of tetrahydroxycalix[4]arene **1** with ethyl bromoacetate to yield tri-functionalized compound **2a** (Scheme 1, Route A). Although selective trialkylation of tetrahydroxycalix[4]arenes had been reported in the presence $Ba(OH)_2 \cdot 8H_2O$ and BaO [20], attempts using similar conditions to convert **1** with ethyl bromoacetate into **2a** resulted in incomplete conversion and concomitant hydrolysis of the ester groups, which has also been observed by Shimizu et al. [21]. To avoid ester hydrolysis, the condensation was repeated with BaO only without the addition of $Ba(OH)_2 \cdot 8H_2O$, which gave **2a**, but only in poor yield (12%) due to complications in the extraction process possibly arising from complex-formation with BaO. When CaH_2 was used as the base, no ester cleavage was observed but the conversion of the reaction was incomplete and mainly bis-alkylated material was isolated. To check the principal feasibility of the first approach, intermediate **2a** was reacted with 4-bromobut-1-yne in the presence of K_2CO_3 and NaI in acetonitrile under reflux. Disappointingly, however, the reaction did not proceed and only starting material was recovered.

Since preparation of the alkyne-functionalized key intermediate **3** via the originally devised route was not successful due to insufficient reactivity of 4-bromobut-1-yne in the final alkylation step, it was decided to switch to an alternative approach based on selective monoalkylation with 4-bromobut-1-yne in the first step, and subsequent alkylation of the remaining hydroxyl-groups with ethyl bromoacetate (Scheme 1, Route B). Employing published procedures for monoalkylation of tetrahydroxycalix[4]arene **1** with benzyl bromide [22] and various alkyl halides [23], reaction with 4-bromobut-1-yne proved to be very slow. To increase the yield and prevent formation of bis-alkylated material, 4-iodobut-1-yne was used instead of 4-bromobut-1-yne, and a number of different bases (K_2CO_3, KO*t*Bu, NaOMe) and solvents (acetonitrile, DMF) were tested. Finally, an optimized procedure was developed comprising addition of multiple portions of NaOMe, which led to a conversion of 49% and allowed isolation of a 3:1 mixture of target compound **2b** (26% isolated yield) and starting material **1**. Since removal of the remaining starting material proved difficult, this mixture was directly used in the next step without further purification. Treatment with excess ethyl bromoacetate in the presence of K_2CO_3 gave compound **3** in 67% yield after repeated purification by silica column chromatography, although the material still contained impurities. The partly purified material was then reacted with *N,N*-dimethylethylenediamine similar to published methods [24], and the crude material purified by preparative HPLC to obtain target compound **4** in a purity of >99%. Copper-catalyzed azide-alkyne cycloaddition (CuAAC) of crude **4** with freshly prepared 2-fluoroethylazide **5** [25] followed by preparative HPLC yielded reference compound **6** in a purity of >99%.

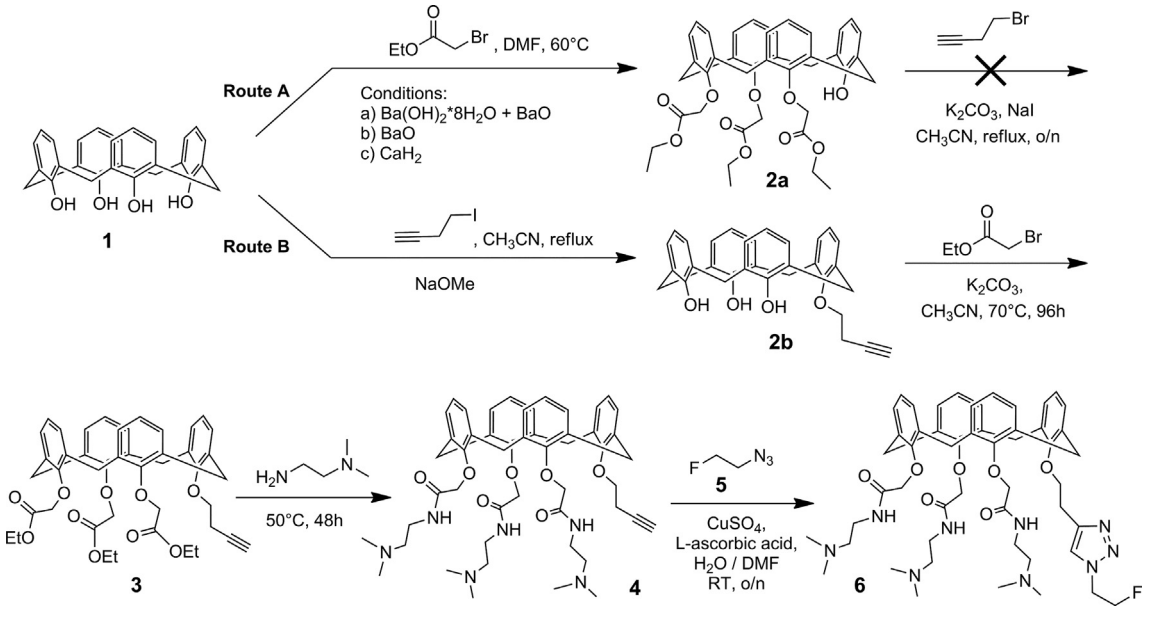

Scheme 1. Synthesis of click precursor **4** and reference compound **6**.

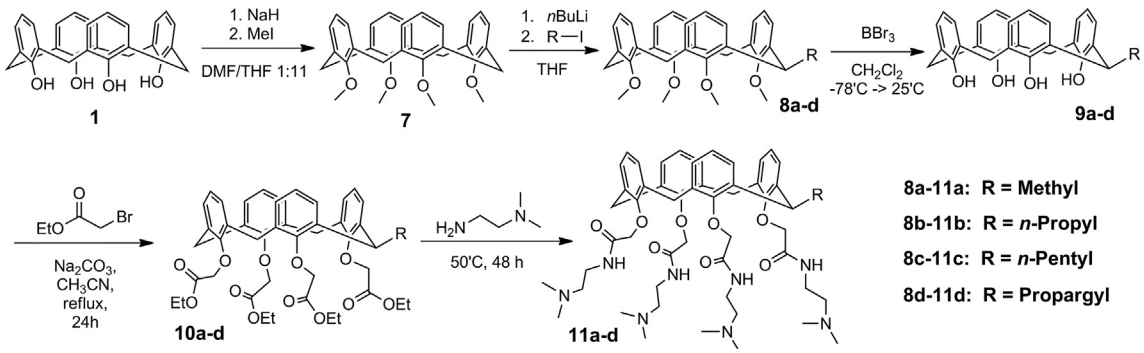

Scheme 2. Synthetic strategy towards equatorially substituted calixarene 0118 analogs.

2.1.2. Synthesis of equatorially substituted compound 0118 analogs

While focus of earlier work in calixarene chemistry was primarily on modification of lower and upper rim positions, fewer reports address the preparation of calixarenes functionalized at the methylene bridge, and synthesis of these compounds was traditionally achieved by fragment condensation instead of introduction of substituents on the fully formed calixarene. The discovery of a new method for monosubstitution of calix[4]arenes at the methylene bridge position via lithiation followed by reaction with electrophiles [26] has made these class of compounds more readily accessible, and triggered us to evaluate its applicability for the preparation of a series of equatorially monosubstituted compound 0118 analogs. Starting directly from tetramethoxycalix[4]arene **7** instead of its upper-rim *p-tert*-butyl analog employed in the original procedure, the desired series of 2-alkyl substituted tetramethoxycalix[4]arenes **8a**–**d** were obtained in good yields from the corresponding alkyl iodides and propargyl bromide, respectively (Scheme 2). Interestingly, a lower excess of *n*-BuLi (1.15 equiv) as employed in a more recent report [27] resulted in significantly lower yields for the present series of compounds, and efficient reaction apparently did only occur when using a large excess of *n*-BuLi (4.5 equiv.) and alkyl halide (9 equiv.) as described in the original work [26]. Removal of the methoxy-protecting groups with BBr_3 yielded 2-alkyl-25,26,27,28-tetrahydroxycalix[4]arenes **9a**–**d**, which were reacted with excess ethyl bromoacetate in the presence of Na_2CO_3 to the corresponding tetraacetates **10a**–**d**. While in previously reported procedures [22,28,29], K_2CO_3 was used as the base, we found that Na_2CO_3 favors formation of the desired cone conformer in higher yields. Final isolated yields, however, were on average only about 30% due to substantial losses during purification by silica column chromatography, which was required to obtain the compounds in high purity. Reaction with *N,N*-dimethylethylenediamine [24] afforded the corresponding compound 0118 analogs **11a**–**d** in 80–99% yield and >90% purity. In summary, starting from tetrahydroxycalix[4]arene **1**, the 5-step synthetic pathway provided the equatorially monoalkylated 0118 analogs **11a**–**d** in overall yields ranging from 11% to 24%. To ensure high purity (>99%) of the test compounds for the biological assays, part of the material was further purified by preparative HPLC.

2.1.3. Synthesis of a compound 0118 analog with a single equatorial triazole moiety and a triazole-PEG-tethered 0118 dimer

Copper-catalyzed azide-alkyne cycloaddition of propargyl-modified 0118 derivative **11d** with 2-fluoroethylazide **5** cleanly provided the corresponding triazole analog **13** in 72% yield, and an analogous procedure using di-azide **12** (0.5 equiv with respect to alkyne **11d**) furnished the PEG_3-tethered 0118 dimer **14**, which was obtained in 47% yield after direct purification of the reaction mixture by preparative HPLC (Scheme 3). This result is in agreement with an earlier report employing Sharpless' conditions [30] with a lower-rim monopropargyl calix[4]arene [31], while difficulties were encountered when using these conditions for lower-rim tetrapropargyl calix[4]arenes [29].

2.2. Cytotoxicity studies (cell viability studies)

Functional efficacy of the new analogs in terms of cytotoxicity and inhibition of cell proliferation was assessed by employing a colorimetric cell viability assay (for details, see Section 4.2). Dose-response curves obtained after incubation of human MA148 ovarian carcinoma cells and HUVEC with increasing concentrations of the analogs are expressed as the percentage of cell survival

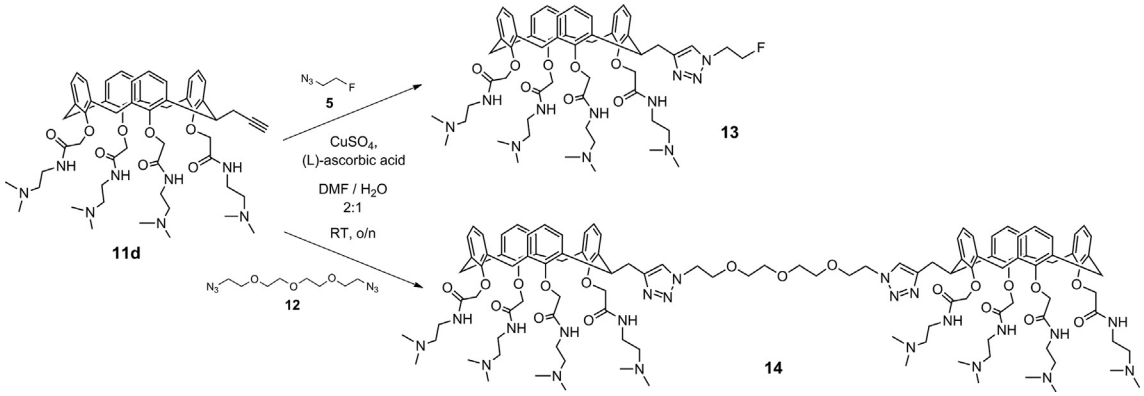

Scheme 3. CuAAC-reaction for preparation of reference compound **13** and calixarene 0118 dimer **14**.

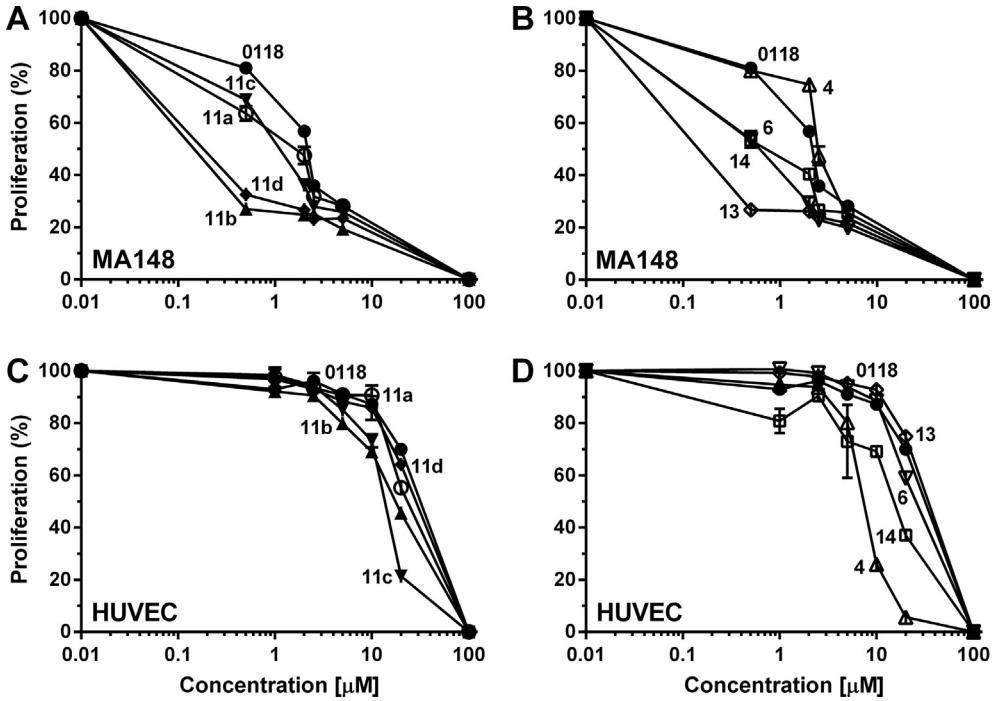

Fig. 2. Effect of new compound 0118 analogs on cell viability of MA148 human ovarian carcinoma cells (A, B) and HUVEC (C, D) as assessed by a colorimetric assay (see Section 4.2 in the experimental section). Data are reported as mean ± SEM relative to untreated control (100%).

Table 1
IC_{50} values (μM) of new 0118 analogs on cell viability.

	0118	**11a**	**11b**	**11c**	**11d**	**13**	**14**	**4**	**6**
HUVEC	30	25	20	15	30	30	15	8	30
MA148	2	1.5	0.2	1	0.2	0.2	0.8	2.5	0.5

relative to control with vehicle only (Fig. 2). The inhibitory potency of the analogs may be compared based on their respective IC_{50} values extrapolated from these curves, which are summarized in Table 1. Results indicate that while all of the new 0118 calixarene analogs are at least equipotent to parent 0118, some of them do inhibit HUVEC and MA148 cell survival almost 4- and 10-fold more potently. All of the equatorially mono-alkylated calixarenes decrease cell viability more effectively than does the parent compound, with potency in the HUVEC-series increasing with increasing alkyl chain length from the methyl-substituted derivative **11a** to the pentyl-substituted derivative **11c**. Calixarenes **6** and **13**, the cold analogs of radiotracers [^{18}F]**6** and [^{18}F]**13**, were found to share a similar inhibition pattern, i.e., IC_{50}-values for HUVEC cell growth were comparable to parent compound 0118, while both analogs showed improved potency towards MA148 cell growth. Furthermore, for both cell lines, the PEG3-linked calixarene dimer **14** only results in slightly more than twice the inhibitory effect of the monomeric 0118.

2.3. Radiochemistry

Radiolabeled compound 0118 derivatives [^{18}F]**6** and [^{18}F]**13** (Fig. 1) were prepared in a two-step reaction sequence (Scheme 4) involving radiosynthesis of the intermediate 2-[^{18}F]fluoroethylazide [^{18}F]**5** followed by CuAAC click coupling to the corresponding alkyne-modified calix[4]arenes **4** (Scheme 1) and **11d** (Schemes 2 and 3), respectively. The labeling agent 2-[^{18}F]fluoroethylazide was prepared by nucleophilic fluorination of 2-azidoethyl-4-toluenesulfonate (**15**) [32] in an automated system using a slightly modified procedure based on previously published methods [25,33]. After purification by co-distillation with acetonitrile at 90 °C under a flow of argon into a receiver vial pre-cooled to −40 °C, 2-[^{18}F]fluoroethylazide [^{18}F]**5** was obtained in 53 ± 5%

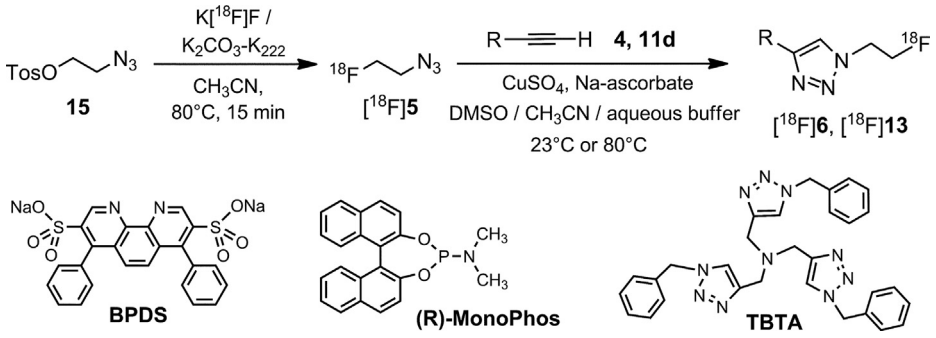

Scheme 4. Radiosynthesis of F-18 labeled calixarenes [^{18}F]**6** and [^{18}F]**13**, and chemical structure of ligands employed in the CuAAC-reaction.

($n = 10$) decay-corrected isolated radiochemical yield starting from [^{18}F]fluoride in a total synthesis time of 60 min.

Conditions for the click reaction with propargyl-calix[4]arene **11d** were optimized in terms of reaction time, temperature, amount of $CuSO_4$/Na-ascorbate, and addition of the Cu(I)-stabilizing ligands BPDS, TBTA, and Monophos (Table 2). Initial test reactions based on the procedure of Kobus et al. [33] using 0.5 equiv. of $CuSO_4$ and 5 equiv. of Na-ascorbate with respect to alkyne **11d** showed maximum conversions after 15 min of less than 10% at 23 °C and about 40% at 80 °C (Table 2, entries 1 and 9). Intrigued by the dramatic rate accelerations reported for CuAAC-reactions in the presence of BPDS [34–36], TBTA [34,36], and MonoPhos [37], we set out to investigate the effect of these ligands (Scheme 4) on the click reaction of [^{18}F]**5** with propargyl-calix[4]arene **11d**. Using conditions identical to the initial test reactions without ligand (Table 2, entries 1 and 9), at 23 °C, only addition of TBTA led to a noteworthy increase in reaction rate (Table 2, entry 4 versus entry 1), while at 80 °C both TBTA and BPDS resulted in similar improvement of analytical yield from about 40% without ligand to >60% with addition of ligand after 15 min (Table 2, entries 12 and 10 versus entry 9). Still, for ^{18}F-radiolabeling using click chemistry, preferably >90% analytical yields should be obtained within reaction times up to 15 min. As an alternative option, we therefore investigated whether higher rate accelerations could be obtained by increasing the copper concentration. Indeed, using a 3-fold molar excess of $CuSO_4$ with respect to alkyne precursor **11d**, almost 5 times higher analytical yields were obtained at room temperature (Table 2, entry 6 versus entry 1), and essentially quantitative product formation was observed at 80 °C, both with alkyne precursor **11d** (Table 2, entry 14 and 15) and with alkyne precursor **4** (Table 2, entry 16).

Interestingly, when using an aqueous solution of alkyne precursor **11d** instead of the DMSO stock solution, the room temperature reaction apparently did not proceed at all (Table 2, entry 7). Although water is generally known to accelerate the CuAAC reaction [30,37,38], in this particular case, DMSO apparently plays an important role as a co-solvent. While large rate accelerations in the presence of BPDS have also been reported at pH 5 [35], in a systematic study comparing performance of various CuAAC-ligands at different pH-values, Lewis et al. [36] have observed fastest rates with BPDS at pH 8.5. Intrigued by their findings, we investigated whether quantitative yields could be obtained for our system using BPDS in the same buffer (Tris/HCl) at pH 8.5. Albeit at room temperature, yields for the reaction with 0.5 equiv. $CuSO_4$ triplicated when employing Tris/HCl-buffer pH 8.5 instead of phosphate buffer pH 6.0 (Table 2, entry 5 versus entry 2), just the opposite trend was observed at 80 °C, where yields dropped down to about 10%, far below the 64% yield obtained with phosphate buffer (Table 2, entry 13 versus entry 10), presumably due to competing side reactions with Tris base at the higher temperature. Although quantitative yields were obtained with the Tris-based buffer system at ambient temperature when increasing the $CuSO_4$/alkyne and BPDS/alkyne molar ratio to 3 and 3.3, respectively (Table 2, entry 8), analytical HPLC-data of the crude reaction mixtures showed a cleaner reaction profile of the ligand-free reaction at 80 °C (Table 2, entry 14) compared to the ligand supported reaction at room temperature. We therefore decided to employ the ligand-free reaction for routine production of the tracers for animal studies on our automated system.

In the semi-automated procedure, 2-[^{18}F]fluoroethylazide [^{18}F]**5** was directly distilled into the pre-cooled receiver vial already containing the DMSO-solution of alkyne precursors **11d** and **4**, respectively. As soon as distillation was complete, the receiver vial was quickly warmed to room temperature, and the freshly made aqueous $CuSO_4$/Na-ascorbate solution was manually added immediately after its preparation. Following reaction for 15 min at 80 °C while stirring with a magnetic stirring bar, the mixture was diluted with water acidified with 0.1% TFA, and injected into the semi-preparative HPLC system. In a number of experiments, radiochemical conversion was determined by analytical HPLC of the diluted crude reaction mixture. Different from the quantitative conversions observed in the test reactions (Table 2, entry 14), yields were sometimes lower and more variable (Table 2, entry 15), which is possibly related to differences in the acetonitrile concentration of the click reaction mixture arising from subtle inter-experimental variations in the distillation step, confirming earlier reports on the negative effect of

Table 2
Optimization of CuAAC conditions – effect of temperature, ligands, catalyst load, and reaction time.[a]

Entry	T (°C)	$CuSO_4$/Na-asc. (equiv.)	Ligand (equiv.)	Buffer (pH)	Analytical yield (%) at:	
					15 min	30 min
1	23	0.5/5	–	Phosphate (6.0)	8.3	16.1
2	23	0.5/5	BPDS (0.55)	Phosphate (6.0)	7.7	10.7
3	23	0.5/5	MonoPhos (0.55)	Phosphate (6.0)	0.2	0.4
4	23	0.5/5	TBTA (0.55)	Phosphate (6.0)	19.4	35.2 ± 2.4[b]
5	23	0.5/5	BPDS (0.55)	Tris/HCl (8.5)	26.4 ± 3.2[b]	43.0 ± 0.3[b]
6	23	3/30	–	Phosphate (6.0)	38.4	67.5
7[f]	23	3/30	–	Phosphate (6.0)	1.1 ± 0.4[b]	1.8 ± 0.2[b]
8	23	3/30	BPDS (3.30)	Tris/HCl (8.5)	98.7	98.5
9	80	0.5/5	–	Phosphate (6.0)	42.2 ± 2.8[c]	52.1 ± 8.5[c]
10	80	0.5/5	BPDS (0.55)	Phosphate (6.0)	63.7 ± 1.3[d]	71.8 ± 7.6[d]
11	80	0.5/5	MonoPhos (0.55)	Phosphate (6.0)	45.2 ± 9.0[d]	73.2 ± 10.3[d]
12	80	0.5/5	TBTA (0.55)	Phosphate (6.0)	65.4	78.9
13	80	0.5/5	BPDS (0.55)	Tris/HCl (8.5)	9.6 ± 1.5[b]	12.2 ± 2.0[b]
14	80	3/30	–	Phosphate (6.0)	98.9 ± 0.2[b]	–
15[g]	80	3/30	–	Phosphate (6.0)	88.1 ± 10.2[c]	–
16[g,h]	80	3/30	–	Phosphate (6.0)	87.5 ± 11.6[e]	–

[a] Unless noted otherwise, all reactions were carried out by adding 2-[^{18}F]fluoroethylazide [^{18}F]**5** in acetonitrile (150 μL) to a solution of 2-propargyl-calix[4]arene **11d** (1.5 μmol) and the indicated ligand in either DMSO or DMSO-H_2O, followed by addition of an aqueous $CuSO_4$/Na-ascorbate solution, which was prepared immediately before use by pre-mixing the appropriate stock solutions of $CuSO_4$ in H_2O and Na-ascorbate in either 0.5 M sodium phosphate buffer pH 6.0 or 0.5 M Tris/HCl-buffer pH 8.5. Total volume of DMSO in the reaction mixtures was 250 μL, total volume of water 125 μL, and buffer concentration in the final mixture was ca. 47 mM. Reaction mixtures were stirred with a magnetic stirring bar.
[b] $n = 2$.
[c] $n = 4$.
[d] $n = 3$.
[e] $n = 5$.
[f] Reaction mixture contained water (250 μL) instead of DMSO (250 μL).
[g] Results obtained using the semi-automated radiosynthesis procedure for routine production of the tracers (3 μmol of **4** or **11d** in 500 μL of DMSO, 250 μL of buffered aqueous $CuSO_4$/Na-ascorbate solution, [^{18}F]**5** in acetonitrile, ca. 300–400 μL, directly distilled onto the precursor solution in DMSO).
[h] Reaction with 28-(3′-butynyloxy)calix[4]arene **4** instead of **11d**.

higher acetonitrile concentrations on radiochemical conversions in the CuAAC reaction [35]. Finally, the product fraction from the semi-preparative HPLC-run was collected, trapped on a C8-SepPak, and formulated in ethanol to obtain radiotracers [^{18}F]**6** and [^{18}F]**13** in overall decay-corrected isolated radiochemical yields of 18.7 ± 2.7% ($n = 4$) and 10.2 ± 5.0% ($n = 4$), respectively. Radiochemical purity of both tracers was always >97% and specific activity generally >5 GBq/μmol. Typically, 400–700 MBq of formulated radiotracers were obtained from 6 to 8 GBq of [^{18}F]F$^-$ eluted from the QMA-cartridge in a total synthesis time of less than 2 h.

2.4. Distribution coefficient and radiotracer stability

Log *D*-values in 1-octanol/PBS pH 7.4 as determined by the shake flask method were +0.8 and −0.1 for the lower-rim and upper-rim [^{18}F]fluoroethyltriazole-substituted compound 0118 analogs [^{18}F]**6** and [^{18}F]**13**, respectively. Evidently, at pH 7.4, the presence of an additional lower-rim substituent containing a protonatable trialkylamino-group results in an approximate 10-fold reduced lipophilicity of [^{18}F]**13** compared to [^{18}F]**6**.

Both radiotracers proved highly stable in PBS pH 7.4 and mouse serum at 37 °C. After incubation of either [^{18}F]**6** or [^{18}F]**13** for 3 h, more than 98% of intact tracer was found both in PBS and mouse serum. Tracer binding to serum proteins after acetonitrile precipitation was negligible, as over 94% of total radioactivity was recovered in the supernatant of the mouse serum samples after centrifugation.

2.5. Biodistribution and dynamic PET studies

For an initial assessment of tumor targeting potential and their pharmacokinetic profile, preliminary *in vivo* studies with radiolabeled 0118 analogs [^{18}F]**6** and [^{18}F]**13** were conducted in mice bearing galectin-1 expressing MDA-MB-231-LITG tumors. Biodistribution results obtained 3 h after intravenous injection of [^{18}F]**6** (0.2–0.3 MBq, corresponding to about 60 ng (63 pmol) of **6**) and [^{18}F]**13** (0.3–0.4 MBq, corresponding to about 100 ng (94 pmol) of **13**) indicate highest uptake of both tracers in the liver, followed by spleen, kidneys, lung, and bone, with only low retention in other organs, including the tumor (Fig. 3A). Evidently, the hepatobiliary route plays an important role for the clearance of both tracers, with the higher accumulation of [^{18}F]**6** in the intestine suggesting faster hepatobiliary excretion of this radiotracer compared to [^{18}F]**13** (Fig. 3B and Supplementary Table 2). Conversely, as a result of the slower excretion of [^{18}F]**13** from the liver and the faster clearance from blood (after 3 h, blood levels of [^{18}F]**6** were 0.76 ± 0.09 %ID/g versus 0.05 ± 0.01 %ID/g for [^{18}F]**13**), radioactivity levels in the liver are almost threefold higher for [^{18}F]**13** compared to [^{18}F]**6** (Fig. 3A). Further differences between the tracers include the almost twofold higher uptake of [^{18}F]**6** in the lung, while [^{18}F]**13** leads to about twofold higher bone uptake, suggesting faster radiodefluorination of the tracer *in vivo* (Fig. 3A). Blood clearance of [^{18}F]**6** (~3.5 MBq, ca. 1 μg of **6**) and [^{18}F]**13** (~8.5 MBq, ca. 1 μg of **13**) followed bi-phasic exponential decay kinetics, with short initial half-lives ($t_{1/2,\alpha}$) of 1.2 min and 1.6 min, and a subsequent slower elimination phase with $t_{1/2,\beta}$ of 74 min and 12 min, respectively (Fig. 3C and Supplementary Table 3). For both tracers, the major part was cleared from the blood by distribution to tissues and extravascular spaces in the α-phase (63% for [^{18}F]**6** versus 79% for [^{18}F]**13**). The slower blood clearance of [^{18}F]**6** in the elimination phase is paralleled by the higher lipophilicity of this tracer, presumably giving rise to increased plasma protein binding [39]. Alternatively, the slower clearance may partly be due to enterohepatic recycling, i.e., intestinal reabsorption of the tracer after biliary excretion [40], a mechanism supported by the predominant and fast hepatobiliary clearance of [^{18}F]**6** (Fig. 4A). Interestingly, biodistribution data (3 h post injection) revealed that the higher dose of cold compound administered for the blood kinetics study (1 μg versus 0.1 μg), resulted in a 25% reduced liver uptake of [^{18}F]**13**, while at the same time kidney uptake was doubled (Supplementary Table 1).

To assess whether higher tumor uptake and tumor-to-organ ratios could be obtained at earlier time points, we conducted dynamic PET-CT studies. PET-images were reconstructed starting from 5 min post tracer injection in timeframes of 5 × 1 min, 4 × 5 min, 3 × 10 min, and 3 × 20 min. Following co-registration of PET- and CT-scans and identification of VOIs in tumor and muscle based on manual segmentation of the CT-images, tracer levels in both tissues were quantified for the different timeframes. Calculated tumor-to-muscle ratios based on these values were below 1 for [^{18}F]**6** and between 1.5 and 2 in case of [^{18}F]**13** for all timeframes investigated. Notably, the more rapid hepatobiliary clearance of [^{18}F]**6** compared to [^{18}F]**13** noted in the biodistribution studies was confirmed in the dynamic PET-scans, which showed immediate uptake in the liver, followed by redistribution to the gallbladder and substantial accumulation of [^{18}F]**6** in the intestines already after 30 min (Fig. 4A). In contrast, intestinal uptake of the more hydrophilic [^{18}F]**13** was slower, while at the same time excretion via the bladder was more pronounced (Fig. 4B).

3. Conclusion

We have designed two close mimetics of galectin-1 targeting antitumor agent calixarene 0118 amenable to radiolabeling with 2-[^{18}F]fluoroethylazide via straightforward click chemistry. Following optimization of reaction conditions and translation to a semi-automated procedure, the lower-rim radiolabeled [^{18}F]**6** and the equatorially modified [^{18}F]**13** were obtained in 18.7 ± 2.7% ($n = 4$) and 10.2 ± 5.0% ($n = 4$) decay-corrected isolated radiochemical yield and >97% radiochemical purity after semi-preparative HPLC purification and formulation. *In vitro* stability studies in mouse serum indicated only negligible binding to serum proteins and excellent stability. Preliminary *in vivo* studies in mice bearing galectin-1 expressing MDA-tumor xenografts showed highest uptake of both tracers in the liver, followed by spleen, kidneys, lung and bone, with only low retention in other organs, including the tumor. Nevertheless, these new radiotracers may become a valuable tool for pharmacokinetic profiling and further development of this class of calixarene-based therapeutics in the future.

Building on the synthetic methodology developed for preparation of the cold reference compounds of the radiotracers (**6**, **13**) and their precursors (**4**, **11d**), we also created a small series of 0118 analogs (**11a**–**c**) containing a single alkyl substituent at an equatorial position on one of the methylene groups, and a PEG_3-spaced calixarene dimer (**14**). Characterization of these eight 0118 derivatives in terms of cytotoxicity and anti-proliferative effects on HUVEC cells and MA148 human ovarian carcinoma cells indicated that all analogs were at least equipotent to lead compound 0118, while some of them were almost 4- to 10-times more potent inhibitors of HUVEC- and MA148 cell growth, respectively. As such, the new analogs may hold potential as a new generation anti-angiogenic agents in cancer therapy with improved potency.

4. Experimental

4.1. Chemistry

4.1.1. General methods and materials

All reagents and solvents were obtained from commercial sources (Sigma–Aldrich, Acros, Biosolve, Merck, and Cambridge

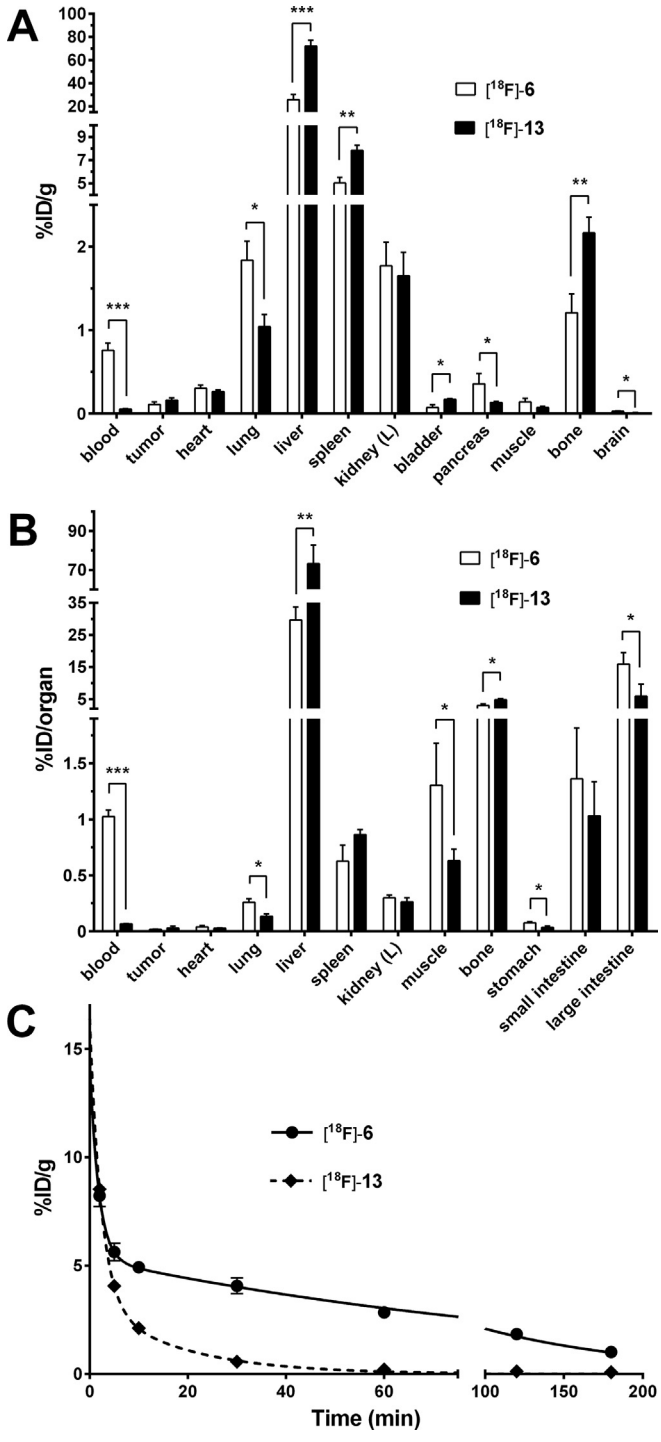

Fig. 3. *Ex vivo* biodistribution and blood clearance: Uptake of radiotracers [^{18}F]**6** (0.2–0.3 MBq, ca. 60 ng of **6**) and [^{18}F]**13** (0.3–0.4 MBq, ca. 100 ng of **13**) in selected organs and tissues of mice bearing MDA-MB-231-LITG tumor xenografts 3 h after intravenous injection, expressed as percentage of injected dose per gram of tissue (%ID/g) (A), and percentage of injected dose per organ (%ID/organ) (B); stomach, small and large intestines were measured including content. Blood clearance of [^{18}F]**6** (~3.5 MBq, ca. 1 μg) and [^{18}F]**13** (~8.5 MBq, ca. 1 μg) fitted to a two-phase exponential decay function (C). Data are mean ± SD ($n = 3$; *$P < 0.05$; **$P < 0.005$; ***$P < 0.0005$).

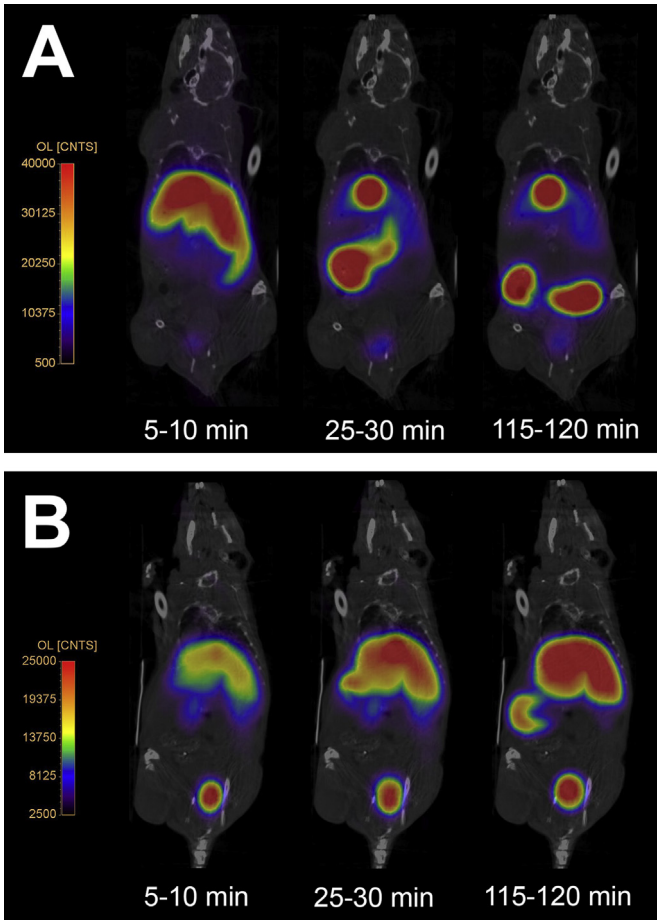

Fig. 4. Dynamic PET-scans: Whole-body PET/CT-images of mice bearing MDA-MB-231-LITG tumor xenografts in the left hind leg. Mice were injected with 12–13 MBq of [^{18}F]**6** (A) or [^{18}F]**13** (B), and list-mode PET data was reconstructed for the indicated timeframes. PET-data in the images are maximum intensity projections.

Isotope Laboratories for deuterated solvents) and were used without further purification unless stated otherwise. 25,26,27,28-Tetrahydroxy-calix[4]arene **1** was from Carbosynth Limited (UK), 1,11-diazido-3,6,9-trioxaundecane **12** from Toronto Research Chemicals Inc. (Canada), and 2-fluoroethyl 4-methylbenzenesulfonate (precursor of **5**) was from Molekula (UK). Unless stated otherwise, all reactions were performed in dried glassware under nitrogen atmosphere. NMR spectra were recorded on a Bruker DPX300, a Bruker Avance600, a Varian VNMRS spectrometer, or a Varian MP300 spectrometer. Chemical shift values are reported in δ (ppm) relative to tetramethylsilane as the internal standard (TMS: $\delta = 0$ ppm for ^{1}H and $\delta = 0$ ppm for ^{13}C), or referenced to the residual solvent peaks ($CDCl_3$: δ 7.26 for ^{1}H and δ 77.0 for ^{13}C). ^{1}H NMR multiplicities are abbreviated as follows: s = singlet, d = doublet, t = triplet, q = quartet, dd = doublet of doublets, dt = doublet of triplets, bs = broad singlet. ^{13}C NMR multiplicities (q = quaternary, t = tertiary, s = secondary, and p = primary) were distinguished using a DEPT pulse sequence or an attached proton test (APT). Preparative column chromatography was performed on a Combiflash Companion apparatus (Teledyne Isco) employing pre-packed silica cartridges from Grace (USA). High-resolution ESI mass spectra (HRMS) were recorded on an Agilent ESI-TOF mass spectrometer.

Preparative HPLC was performed on two different systems. System A: Agilent 1200 apparatus, equipped with a C18 Zorbax column (21.2 × 150 mm, 5 μm) applying a linear gradient of acetonitrile (B) in water (A), both containing 0.1% TFA. Gradient details: 30% B (0 min → 5 min), 30% B → 50% B (5 min → 12 min), 50% B (12 min → 15 min), 50% B → 95% B (15 min → 16 min), 95% B (16 min → 18 min), 95% B → 30% B (18 min → 19 min), 30% B

(19 min → 22 min). Flow: 10 mL/min. Injection volume: 0.5 mL. UV detection: 215 nm, 254 nm. System B: Instrument: Agilent 1100 series, equipped with a Gemini NX C_{18} 100A Axia column (30 × 100 mm, 5 μm) employing a linear gradient of acetonitrile (B) in aqueous 20 mM ammoniumbicarbonate (A). Gradient details: 50%B (0 min → 3 min), 50% B → 95% B (3 min → 9 min), 95% B (9 min → 10 min). Flow: 40 mL/min. Injection volume: 25 μL. UV detection: 215 nm, 254 nm.

Analytical HPLC–MS was carried out on System C: Agilent 1100 series with UV detector and HP 1100 mass TOF detector, equipped with a Kinetex C18 (50 × 2.10 mm; 2.6 μm) column, variable wavelength UV-detector, and API ES TOF positive and negative mass detection. Column temperature: 35 °C. Flow: 0.60 mL/min. Injection volume: 1 μL. Mobile phase: 9.65 g ammonium acetate, 2250 mL H_2O, 150 mL methanol, 100 mL acetonitrile (eluent A); 9.65 g ammonium acetate, 250 mL H_2O, 1350 mL methanol, 900 mL acetonitrile (eluent B).

4.1.2. 25,26,27-Trihydroxy-28-(3′-butynyloxy)calix[4]arene (**2b**)

To 25,26,27,28-tetrahydroxycalix[4]-arene **1** (4 g, 9.42 mmol) in acetonitrile (220 mL) was added freshly prepared NaOMe (600 mg, 11.12 mmol). The mixture was refluxed for 30 min, cooled and 4-iodobut-1-yne (3.29 g, 24 mmol) in acetonitrile (40 mL) was added (4-iodobut-1-yne was freshly prepared from NaI (7.2 g, 48 mmol) and 4-bromobut-1-yne (3.2 g, 24 mmol) in acetonitrile (40 mL) at reflux for 1 h). The mixture was refluxed overnight and the conversion was checked by ^{1}H NMR (24%). Additional NaOMe (400 mg, 7.41 mmol) was added and the mixture was refluxed over the weekend (conversion 32%). Additional NaOMe (400 mg, 7.41 mmol) was added and the mixture was stirred at reflux for another 48 h. NMR analysis showed a conversion of 39%. Then additional freshly prepared NaOMe (400 mg, 7.41 mmol) was added and the mixture was refluxed for another 48 h. Conversion (49%) and also 5% bis-alkylated material was formed. Then the mixture was worked up by evaporation of the solvent. Dichloromethane (100 mL) was added to the residue and the mixture was washed with water (3 × 50 mL). After evaporation of the organic solvents an off-white solid was isolated. The title compound was isolated as a mixture with unreacted 25,26,27,28-tetrahydroxycalix[4]arene. The material was stirred in ethyl acetate (15 mL) and the solid was filtered. The mother liquor was evaporated and 1.5 g of crude product was isolated. According to ^{1}H NMR this sample contains approx. 75% of the title compound (corresponding to 1.16 g, 2.43 mmol, 26% yield of **2b**) and 25% of starting material. The solid was used in the next step without further purification. ^{1}H NMR (300 MHz, $CDCl_3$) δ 9.7 (s, 1H), 9.17 (s, 2H), 7.09 (m, 8H), 6.90 (m, 1H), 6.69 (m, 3H), 4.43 (d, 2H, ^2J = 13.0 Hz), 4.29 (m, 4H), 3.49 (d, 4H, ^2J = 12.9 Hz), 3.06 (dt, 2H, ^4J = 2.7 Hz, ^3J = 6.6 Hz), 2.23 (t, 1H, ^4J = 2.7 Hz). ^{13}C NMR (75 MHz, $CDCl_3$) δ 151.32 (q), 151.05 (q), 149.45 (q), 134.34 (q), 129.69 (q), 129.23 (q), 129.11 (q), 129.02 (q), 128.66 (q), 128.59 (t), 128.49 (t), 126.58 (q), 122.20 (t) 121.15 (t), 80.42 (q), 74.60 (t), 71.28 (s), 32.15 (s), 31.66 (s), 20.35 (s).

4.1.3. 25,26,27-Tri[(ethoxycarbonyl)methoxy]-28-(3′-butynyloxy) calix[4]arene (**3**)

To a solution of **2b** (1.5 g with purity 75%, corresponding to 2.43 mmol of **2b**) in acetonitrile (20 mL) was added K_2CO_3 (964 mg, 6.98 mmol). The mixture was stirred for 30 min and then an excess of ethyl bromoacetate (2.63 g, 15.75 mmol) was added. The mixture was heated to 70 °C for 96 h. After cooling, the acetonitrile was evaporated. The residue was taken up in dichloromethane (100 mL). The organic layer was washed with water (2 × 50 mL). After separation the organic layer was evaporated. The impure compound was purified by column chromatography (silicagel, dichloromethane). Several impure fractions were isolated. The first combined fractions (900 mg) contained product and by-products. The second batch of combined fractions was enriched in product (1 g) and the third batch (500 mg) was a combination of fractions which contained mainly tetraethyl ester. The first batch was purified by column chromatography again on silicagel with dichloromethane to remove by-products and then ethyl acetate:heptanes = 1:2 to elute the product. Approximately 450 mg of a mixture was isolated which was enriched in product. This material was combined with the 1 g batch. A total of 1.45 g of material was purified again by silica column chromatography using a mixture of ethyl acetate:heptanes = 6:1 followed by ethyl acetate:heptanes = 4:1 to obtain the title compound (1.2 g, 1.63 mmol, 67%). Unfortunately, ^{1}H NMR analysis still indicated presence of some impurities. A 300 mg batch was used in the next step without further purification. The remainder (900 mg) was again purified by repeated silica column chromatography, first using dichloromethane followed by ethyl acetate:heptanes = 1:4, then toluene:ethyl acetate = 95:5 to obtain the pure title compound (30 mg, 0.04 mmol) and a slightly less pure fraction (260 mg, 0.35 mmol). ^{1}H NMR (300 MHz, $CDCl_3$) δ 6.79–6.68 (m, 6H), 6.57–6.53 (m, 6H), 4.85 (d, 2H, ^2J = 13.6 Hz), 4.80–4.56 (m, 8H), 4.28 (q, 4H, ^3J = 7.2 Hz), 4.24 (q, 2H, ^3J = 7.2 Hz), 4.10 (t, 2H, ^3J = 7.6 Hz), 3.28 (d, 2H, ^3J = 13.3 Hz), 3.22 (d, 2H, ^3J = 13.3 Hz), 2.92 (dt, 2H, ^4J = 2.6 Hz, ^3J = 7.6 Hz), 1.97 (t, 1H, ^4J = 2.6 Hz), 1.27–1.36 (m, 9H). ^{13}C NMR (75 MHz, $CDCl_3$) δ 170.41 (q), 170.11 (q), 156.59 (q), 156.34 (q), 155.53 (q), 135.62 (q), 135.10 (q), 134.61 (q), 134.25 (q), 128.93 (t), 128.77 (t), 128.68 (t), 128.57 (t), 123.07 (t), 122.93 (t), 82.19 (q), 72.74 (s), 71.79 (s), 71.70 (s), 69.36 (t), 60.96 (s), 60.79 (s), 31.48 (s), 31.29 (s), 20.03 (s), 14.50 (p), 14.44 (p). Analytical HPLC–MS (system C), gradient: 20% B → 95% B (0 min → 1.5 min), 95% B (1.5 min → 4.0 min). Retention time: 3.65 min. Purity >99.99% (UV, 215, 254 nm). MS calculated for $C_{44}H_{46}O_{10}$: 734.31; MS (API-ES TOF Pos): m/z 752 $[M+NH_4]^+$, 757 $[M+Na]^+$.

4.1.4. 25,26,27-Tris-N-(N,N-dimethyl-2-aminoethyl) carbamoylmethoxy-28-(3′-butynyloxy)calix[4]arene (**4**)

To powdered **3** (300 mg, 0.41 mmol) was added under nitrogen *N*,*N*-dimethylethylenediamine (5 mL). The mixture was stirred at room temperature for 1 h and was then stirred for 48 h at 50 °C. The excess of *N*,*N*-dimethylethylenediamine was removed by evaporation under reduced pressure. A sample of 220 mg was dissolved in tetrahydrofuran (unstabilized, concentration of crude 70 mg/mL) and purified by preparative HPLC on system B (see general methods). Fractions containing the product (t_R = 6.4 min; broad peak) were pooled and evaporated at the rotary evaporator to remove the acetonitrile. The water was removed by freeze-drying to obtain the pure target compound as an off-white foam (110 mg, 128 μmol, c.y. 38%).

^{1}H NMR (300 MHz, $CDCl_3$) δ 6.74–6.67 (m, 6H), 6.60–6.47 (m, 6H), 4.57 (d, 2H, ^2J = 13.9 Hz), 4.56–4.33 (m, 8H), 4.14 (t, 2H, ^3J = 7.3 Hz), 3.56–3.40 (m, 6H), 3.28 (d, 2H, ^2J = 14.2 Hz), 3.26 (d, 2H, ^2J = 13.8 Hz), 2.75 (dt, 2H, ^4J = 2.7 Hz, ^3J = 7.3 Hz), 2.53 (t, 4H, ^3J = 6.6 Hz), 2.45 (t, 2H, ^3J = 6.5 Hz), 2.26 (s, 12H), 2.20 (s, 6H), 2.09 (t, 1H, ^4J = 2.6 Hz). ^{13}C NMR (75 MHz, $CDCl_3$) δ 169.58 (q), 169.46 (q), 156.11 (q), 155.60 (q), 155.47 (q), 135.21 (q), 134.92 (q), 133.94 (q), 133.80 (q), 129.18 (t), 129.00 (t), 128.85 (t), 128.71 (t), 123.29 (t), 123.22 (t), 81.81 (q), 74.31 (s), 74.15 (s), 72.61 (s), 70.47 (t), 58.31 (s), 58.18 (s), 57.98 (s), 45.51 (p), 45.44 (p), 45.29 (p), 37.26 (s), 37.17 (s), 35.65 (s), 31.32 (s), 31.07 (s), 19.94 (s). Analytical HPLC–MS (system C), gradient: 20% B → 90% B (0 min → 1.0 min), 90% B → 100% B (1.0 min → 3.5 min), 100% B (3.5 min → 4.0 min). Retention time: 2.03 min. Purity 99.64% (UV, 218 nm). MS calculated for $C_{50}H_{64}N_6O_7$: 860.48; MS (API-ES TOF Pos): m/z 431 $[M+2H]^{2+}$, 861 $[M+H]^+$, 883 $[M+Na]^+$; MS (API-ES TOF Neg): m/z 859 $[M-H]^-$, 919 $[M-CH_3COO]^-$.

4.1.5. 25,26,27-Tris-N-(N,N-dimethyl-2-aminoethyl) carbamoylmethoxy-28-{2′-[1-(2-fluorethyl)-1H-[1,2,3]triazo-4-yl] ethyloxy}calix[4]arene (**6**)

To a stirred solution of $CuSO_4 \times 5H_2O$ (21.3 mg, 86 μmol) and L-ascorbic acid (30.3 mg, 172 μmol) in water (1 mL) under an N_2 atmosphere was added a solution of crude **4** (50 mg, 57 μmol) in *N*,*N*-dimethylformamide (0.7 mL). After addition of 2-fluoroethylazide **5** (5.09 mg, 57 μmol in 1 mL of *N*,*N*-dimethylformamide; solution freshly prepared following published procedures [25]), the mixture was stirred at room temperature overnight, and then evaporated to dryness. The solid residue was treated with dichloromethane (5 mL) and water (5 mL). A few drops of NaOH (1 M) were added. The layers were separated and the aqueous layer was again extracted with dichloromethane (5 mL). The combined organic layers were washed with water (5 mL) and evaporated *in vacuo*. The crude material (40 mg) was taken up in tetrahydrofuran (unstabilized, 60 mg/mL, injection volume 25 μL) and purified by preparative HPLC on system B (see general methods). Fractions containing the product ($t_R = 6.8$ min; broad peak) were pooled and evaporated at the rotary evaporator to remove the acetonitrile. The water was removed by freeze-drying. The target compound was isolated as a white solid 15 mg (15.7 μmol, c.y. 27.7%). A larger batch (50 mg) has been synthesized in the same way. ^{1}H NMR (300 MHz, $CDCl_3$) δ 7.96 (m, 1H), 7.64 (m, 2H), 7.60 (s, 1H), 6.67 (s, 6H), 6.59–6.41 (m, 6H), 4.79 (dt, $^2J_{HF} = 46.9$ Hz, $^3J_{HH} = 4.6$ Hz, 2H), 4.74–4.48 (m, 8H), 4.27 (d, $^2J = 14.2$ Hz, 4H), 4.26–4.18 (m, 2H), 3.55–3.33 (m, 6H), 3.28 (t, $^3J = 6.9$ Hz, 2H), 3.23 (d, $^2J = 13.9$ Hz, 4H), 2.51–2.40 (m, 6H), 2.22 (s, 6H), 2.20 (s, 12H). ^{13}C NMR (75 MHz, $CDCl_3$) δ 169.55 (q), 169.16 (q), 156.33 (q), 145.02 (q), 134.52 (q), 134.27 (q), 134.17 (q), 134.08 (q), 129.30 (t), 128.79 (t) 128.76 (t), 128.49 (t), 123.23 (t), 123.03 (t), 122.92 (t), 122.76 (t), 122.74 (t), 81.54 (s, doublet, $^1J_{CF} = 171$ Hz), 74.49 (s), 73.87 (s), 73.77 (s), 58.27 (s), 58.11 (s), 50.50 (s, doublet, $^2J_{CF} = 20$ Hz), 45.41 (p), 37.14 (s), 31.33 (s), 30.98 (s), 26.76 (s). ^{19}F NMR (282 MHz, $CDCl_3$) δ −150.75 to −151.23 (m, 1F). Analytical HPLC–MS (system C), gradient: 20% B → 95% B (0 min → 1.5 min), 95% B (1.5 min → 4.0 min). Retention time: 2.41 min. Purity 99.82% (UV, 224 nm). MS calculated for $C_{52}H_{68}FN_9O_7$: 949.52; MS (API-ES TOF Pos): *m*/*z* 475 $[M+2H]^{2+}$, 950 $[M+H]^+$.

4.1.6. 25,26,27,28-Tetramethoxycalix[4]arene (**7**)

Compound **7** was prepared as described [41], with minor modifications. Briefly, 25,26,27,28-Tetrahydroxycalix[4]-arene **1** (7.5 g, 17.7 mmol) was dissolved in a 10:1 mixture of anhydrous tetrahydrofuran:*N*,*N*-dimethylformamide (165 mL). NaH (12 g of a 60% dispersion in mineral oil, 300 mmol) was triturated with *n*-pentane to remove the mineral oil. After drying under a gentle stream of nitrogen, the NaH was added to the precursor solution in tetrahydrofuran/*N*,*N*-dimethylformamide, followed by MeI (33 mL, 531 mmol). The reaction mixture was refluxed for 2 h, treated with methanol (10 mL) to decompose the excess of NaH, and evaporated *in vacuo*. The solid was partitioned between water (300 mL) and dichloromethane (300 mL). The layers were separated and the water layer was again extracted with dichloromethane (300 mL). The combined organic layers were back-extracted with water (150 mL), dried on $MgSO_4$, and evaporated *in vacuo*. Traces of MeI and *N*,*N*-dimethylformamide were efficiently removed by coevaporation with dichloromethane. Yield: 8.3 g (17.3 mmol, 98%) of a white to slightly yellow solid. ^{1}H NMR (300 MHz, CD_3CN sat. with NaI) δ 7.34 (d, $^3J = 7.7$ Hz, 8H), 6.92 (t, $^3J = 7.7$ Hz, 4H), 4.28 (d, $^2J = 12.5$ Hz, 4H), 4.14 (s, 12H), 3.60 (d, $^2J = 12.5$ Hz, 4H). ^{13}C NMR (75 MHz, CD_3CN sat. with NaI) δ 153.80(q), 136.33(q) 130.26(t), 126.77(t), 65.58(p), 29.75(s). HRMS (ESI, *m*/*z*): Calculated for $C_{32}H_{32}O_4H^+$ ($[M+H]^+$): 481.2379, Found: 481.2382.

4.1.7. General procedure for preparation of 25,26,27,28-tetramethoxy-2-alkylcalix[4]arenes (**8a**–**d**)

25,26,27,28-Tetramethoxycalix[4]arene **7** (2.00 g, 4.16 mmol) was dissolved in anhydrous THF (100 mL). The clear yellow solution was cooled to −20 °C, and *n*-BuLi (11.7 mL of 1.6 M *n*-BuLi in hexanes, 18.7 mmol) was added dropwise in the course of 30 min. The resulting blood-red solution was allowed to stir for 45 min. Alkyl iodide (37.4 mmol) was added, and the solution, which has turned orange–brown, was allowed to stir for 1 h while warming up to room temperature. After quenching with sat. aq. $KHSO_4$ (20 mL) and evaporation of most of the THF, water (80 mL) was added, and the product was extracted with dichloromethane (2 × 80 mL). The combined organic extracts were washed with brine (80 mL), dried on $MgSO_4$, and filtered over a short column of silica to remove highly polar impurities (baseline spot on TLC), followed by passing an additional 80 mL of dichloromethane, and evaporated *in vacuo*.

*4.1.7.1. 25,26,27,28-Tetramethoxy-2-methylcalix[4]arene (**8a**).* Alkylation with methyl iodide (2.4 mL) yielded the title compound as an off-white solid (1.96 g, 3.96 mmol, 95%). ^{1}H NMR (300 MHz, CD_3CN sat. with NaI) δ 7.41 (dd, $^3J = 7.9$ Hz, $^4J = 1.5$ Hz, 2H), 7.34 (d, $^3J = 7.7$ Hz, 4H), 7.31 (dd, $^3J = 7.7$ Hz, $^4J = 1.5$ Hz, 2H), 6.96 (t, $^3J = 7.7$ Hz, 2H), 6.92 (t, $^3J = 7.7$ Hz, 2H), 4.88 (q, $^3J = 7.5$ Hz, 1H), 4.28 (d, $^2J = 12.5$ Hz, 2H), 4.27 (d, $^2J = 12.5$ Hz, 2H), 4.14 (s, 6H), 4.12 (s, 6H), 3.60 (d, $^2J = 12.5$ Hz, 3H), 1.71 (d, $^3J = 7.5$ Hz, 3H). HRMS (ESI, *m*/*z*): Calculated for $C_{33}H_{34}O_4H^+$ ($[M+H]^+$): 495.2530, Found: 495.2553.

*4.1.7.2. 25,26,27,28-Tetramethoxy-2-propylcalix[4]arene (**8b**).* Alkylation with 1-iodopropane (3.7 mL) yielded the title compound as pale yellow solid (1.82 g, 3.48 mmol, 84%). ^{1}H NMR (300 MHz, CD_3CN sat. with NaI) δ 7.40–7.28 (m, 8H), 6.99–6.88 (m, 4H), 4.69 (t, $^3J = 8.1$ Hz, 1H), 4.27 (d, $^3J = 12.5$ Hz, 3H), 4.14 (s, 6H), 4.12 (s, 6H), 3.60 (d, $^2J = 12.5$ Hz, 2H), 3.59 (d, $^2J = 12.5$ Hz, 1H), 2.20–2.02 (m, 2H), 1.44–1.24 (m, 2H), 0.99 (t, $^3J = 7.2$ Hz, 3H). ^{13}C NMR (75 MHz, CD_3CN sat. with NaI) δ 153.89 (q), 153.79 (q), 140.00 (q), 136.41 (q), 136.37 (q), 136.16 (q), 130.29 (t), 129.89 (t), 126.99 (t), 126.79 (t), 65.68 (p), 65.56 (p), 36.88 (s), 36.04 (t), 29.92 (s), 29.77 (s), 22.60 (s), 14.60 (p). HRMS (ESI, *m*/*z*): Calculated for $C_{35}H_{38}O_4H^+$ ($[M+H]^+$): 523.2843, Found: 523.2818.

*4.1.7.3. 25,26,27,28-Tetramethoxy-2-pentylcalix[4]arene (**8c**).* Alkylation with 1-iodopentane (4.9 mL) yielded the title compound as a white solid (1.91 g, 3.47 mmol, 83%). ^{1}H NMR (300 MHz, CD_3CN sat. with NaI) δ 7.39–7.28 (m, 8H), 6.99–6.88 (m, 4H), 4.67 (t, $^3J = 8.1$ Hz, 1H), 4.27 (d, $^2J = 12.5$ Hz, 3H), 4.14 (s, 6H), 4.11 (s, 6H), 3.60 (d, $^2J = 12.5$ Hz, 2H), 3.59 (d, $^2J = 12.5$ Hz, 1H), 2.20–2.02 (m, 2H), 1.43–1.23 (m, 6H), 0.86 (t, $^3J = 7.2$, Hz, 3H). ^{13}C NMR (75 MHz, CD_3CN sat. with NaI) δ 153.87 (q), 153.79 (q), 140.00 (q), 136.40 (q), 136.35 (q), 136.15 (q), 130.28 (t), 129.89 (t), 126.97 (t), 126.78 (t), 65.66 (p), 65.55 (p), 36.20 (t), 34.51 (s), 32.46 (s), 29.91 (s), 29.75 (s), 29.08 (s), 22.97 (s), 14.26 (p). HRMS (ESI, *m*/*z*): Calculated for $C_{37}H_{42}O_4H^+$ ($[M+H]^+$): 551.3156, Found: 551.3176.

*4.1.7.4. 25,26,27,28-Tetramethoxy-2-(prop-2′-yn-1′-yl)calix[4]arene (**8d**).* Preparation of **8d** was performed using a slightly modified procedure. Briefly, the lithiated intermediate obtained by dropwise addition of *n*-BuLi (7.8 mL of 1.6 M *n*-BuLi in hexanes, 12.5 mmol) to an ice-cooled solution of tetramethoxycalix[4]arene **7** (1 g, 2.08 mmol) in anhydrous tetrahydrofuran (30 mL) was added (almost) at once to a pre-cooled solution (ice bath) of propargyl bromide (2.78 mL of an 80 wt. % solution in toluene, 25.0 mmol) in anhydrous tetrahydrofuran (15 mL). The reaction mixture was stirred for 1 h in an ice-bath, allowed to warm to room temperature (ca. 20 min), and then quenched with saturated aqueous $KHSO_4$

(10 mL) and worked up as described in the general procedure. ^{1}H NMR of the crude product (950 mg) indicated a conversion of ca. 80% (corresponding to 771 mg, 1.49 mmol, 72% yield of pure **8d**). The crude product was purified by column chromatography on silicagel employing a gradient of 0–10% of ethyl acetate in heptanes. Fractions containing the product were pooled, evaporated *in vacuo*, and co-evaporated with dichloromethane to remove traces of heptanes. Yield: 402 mg (0.78 mmol, 37%) of a white solid. ^{1}H NMR (300 MHz, CD_3CN sat. with NaI) δ 7.43 (dd, ^3J = 7.9 Hz, ^4J = 1.4 Hz, 2H), 7.35 (d, ^3J = 7.7 Hz, 6H), 6.97 (t, ^3J = 7.7 Hz, 2H), 6.92 (t, ^3J = 7.7 Hz, 2H), 4.95 (t, ^3J = 8.6 Hz, 1H), 4.28 (d, ^2J = 12.5 Hz, 2H), 4.27 (d, ^2J = 12.5 Hz, 1H), 4.18 (s, 6H), 4.14 (s, 6H), 3.62 (d, ^2J = 12.5 Hz, 2H), 3.60 (d, ^2J = 12.5 Hz, 1H), 3.15 (dd, ^3J = 8.4 Hz, ^4J = 2.5 Hz, 2H), 2.33 (t, ^4J = 2.5 Hz, 1H). ^{13}C NMR (75 MHz, CD_3CN sat. with NaI) δ 153.86 (q), 153.63 (q), 138.38 (q), 136.36 (q), 136.34 (q), 136.30 (q), 130.44 (t), 130.33 (t), 130.29 (t), 127.06 (t), 126.90 (t), 126.83 (t), 83.98 (q), 71.42 (t), 65.91 (p), 65.54 (p), 35.88 (t), 29.90 (s), 29.73 (s), 23.90 (s). HRMS (ESI, *m/z*): Calculated for $C_{35}H_{34}O_4H^+$ ($[M+H]^+$): 519.2535, Found: 519.2561.

4.1.8. General procedure for preparation of 25,26,27,28-tetrahydroxy-2-alkylcalix[4]arenes (**9a**–**d**)

25,26,27,28-Tetramethoxy-2-alkylcalix[4]arene **8a**–**d** (0.7–2.9 mmol) was dissolved in anhydrous dichloromethane (50 mL for **8a**–**c**, 30 mL for **8d**) and cooled to −78 °C. A 1.0 M solution of BBr_3 in dichloromethane (4.8–18.7 mL, 6.5 equiv.) was added dropwise via a syringe, and the resulting mixture was stirred for 1 h at −78 °C, then allowed to warm to room temperature. After 30 min at room temperature, the reaction mixture was quenched by addition of saturated aq. $NaHCO_3$ (50 mL). Layers were separated, and the organic layer was washed with water (50 mL). After drying on $MgSO_4$, the extracts were passed over a thin column of silica, followed by rinsing with dichloromethane (200 mL), and evaporated *in vacuo*. For **9d**, a slightly different workup was employed (see below).

*4.1.8.1. 25,26,27,28-Tetrahydroxy-2-methylcalix[4]arene (**9a**).* Demethylation of **8a** (1.16 g, 2.35 mmol) with 1.0 M BBr_3 in dichloromethane (15.3 mL, 15.3 mmol) yielded the title compound as a white foam (0.776 g, 1.77 mmol, 75%). ^{1}H NMR (300 MHz, $CDCl_3$) δ = 10.15 (s, 4H), 7.18–6.98 (m, 8H), 6.77 (t, ^3J = 7.5 Hz, 2H), 6.72 (t, ^3J = 7.7 Hz, 2H), 4.74 (q, ^3J = 7.2 Hz, 1H), 4.26 (d, ^2J = 13.9 Hz, 1H), 4.25 (d, ^2J = 13.9 Hz, 2H), 3.53 (d, ^2J = 13.9 Hz, 3H), 1.71 (d, ^3J = 7.2 Hz, 3H). HRMS (ESI, *m/z*): Calculated for $C_{29}H_{26}O_4H^+$ ($[M+H]^+$): 439.1904, Found: 439.1895.

*4.1.8.2. 25,26,27,28-Tetrahydroxy-2-propylcalix[4]arene (**9b**).* Demethylation of **8b** (1.50 g, 2.87 mmol) with 1.0 M BBr_3 in dichloromethane (18.7 mL, 18.7 mmol) yielded the title compound as a white foam (1.28 g, 2.74 mmol, 95%). ^{1}H NMR (300 MHz, $CDCl_3$) δ = 10.12 (s, 4H), 7.19–6.88 (m, 8H), 6.80–6.64 (m, 4H), 4.53 (t, ^3J = 7.8 Hz, 1H), 4.26 (d, ^2J = 13.9 Hz, 1H), 4.25 (d, ^2J = 13.8 Hz, 2H), 3.53 (d, ^2J = 13.9 Hz, 3H), 2.22–2.05 (m, 2H), 1.42–1.23 (m, 2H), 0.95 (t, ^3J = 7.3 Hz, 3H). HRMS (ESI, *m/z*): Calculated for $C_{31}H_{30}O_4H^+$ ($[M+H]^+$): 467.2217, Found: 467.2214.

*4.1.8.3. 25,26,27,28-Tetrahydroxy-2-pentylcalix[4]arene (**9c**).* Demethylation of **8c** (720 mg, 1.31 mmol) with 1.0 M BBr_3 in dichloromethane (8.5 mL, 8.5 mmol) yielded the title compound as a white foam (594 mg, 1.20 mmol, 92%). ^{1}H NMR (300 MHz, $CDCl_3$) δ = 10.11 (s, 4H), 7.15–6.95 (m, 8H), 6.80–6.65 (m, 4H), 4.49 (t, ^3J = 7.7 Hz, 1H), 4.26 (d, ^2J = 13.9 Hz, 1H), 4.25 (d, ^2J = 13.9 Hz, 2H), 3.53 (d, ^2J = 13.9 Hz, 3H), 2.22–2.08 (m, 2H), 1.40–1.25 (m, 6H), 0.92–0.83 (m, 3H). HRMS (ESI, *m/z*): Calculated for $C_{33}H_{34}O_4H^+$ ($[M+H]^+$): 495.2530, Found: 495.2508.

*4.1.8.4. 25,26,27,28-Tetrahydroxy-2-(prop-2′-yn-1′-yl)calix[4]arene (**9d**).* Demethylation of **8d** (379 mg, 0.73 mmol) in anhydrous dichloromethane (30 mL) with 1.0 M BBr_3 in the same solvent (4.75 mL, 4.75 mmol), followed by a slightly modified workup (partitioning between 120 mL of sat. aq. $NaHCO_3$ and 120 mL of dichloromethane, washing of the organic layer with 120 mL of water, drying over $MgSO_4$, and evaporation *in vacuo*) yielded the crude title compound in quantitative yield. After purification by silica column chromatography employing a gradient of 5–30% of ethyl acetate in heptanes, the pure target compound was obtained as a white solid (36 mg, 0.078 mmol, 11%). ^{1}H NMR (300 MHz, $CDCl_3$) δ 10.10 (s, 4H), 7.08–7.02 (m, 8H), 6.78 (t, ^3J = 7.7 Hz, 2H), 6.73 (t, ^3J = 7.7 Hz, 2H), 4.85 (t, ^3J = 7.5 Hz, 1H), 4.26 (d, ^2J = 13.9 Hz, 3H), 3.54 (d, ^2J = 13.9 Hz, 3H), 3.07 (d, ^3J = 7.5 Hz, 2H), 1.90 (t, ^4J = 2.4 Hz, 1H). ^{13}C NMR (75 MHz, $CDCl_3$) δ 149.98 (q), 148.96 (q), 130.29 (q), 129.17 (t), 129.09 (t), 129.03 (t), 128.44 (q), 128.33 (q), 128.28 (q), 124.54 (t), 122.61 (t), 122.41 (t), 82.45 (q), 69.56 (t), 35.47 (t), 31.94 (s), 31.84 (s), 22.32 (s). HRMS (ESI, *m/z*): Calculated for $C_{31}H_{26}O_4H^+$ ($[M+H]^+$): 463.1909, Found: 463.1932.

4.1.9. General procedure for preparation of 25,26,27,28-tetra[(ethoxycarbonyl)methoxy]-2-alkylcalix[4]arenes (**10a**–**d**)

25,26,27,28-Tetrahydroxy-2-alk(yn)ylcalix[4]arene **9a**–**d** (0.49–1.61 mmol) was dissolved in dry acetonitrile (15 mL) followed by addition of finely powdered anhydrous Na_2CO_3 (4.9–16.1 mmol, ca. 10 equiv.). The resulting suspension was stirred for 1 h at 30 °C, ethyl bromoacetate (4.9–16.1 mmol, 10 equiv.) was added, and the reaction mixture was refluxed for 20 h. The solvent was evaporated *in vacuo* and the residue partitioned between dichloromethane (30 mL) and water (30 mL). The water layer was extracted with dichloromethane (2 × 15 mL). The combined organic extracts were dried on $MgSO_4$, filtered, and evaporated *in vacuo* to yield the crude product, which was purified by silica column chromatography employing a gradient of 15–30% of ethyl acetate in heptane to obtain the pure target compound. For **10d**, a slightly different workup was employed (see below).

*4.1.9.1. 25,26,27,28-Tetra[(ethoxycarbonyl)methoxy]-2-methylcalix[4]arene (**10a**).* Precursor and reagents: **9a** (367 mg, 0.84 mmol); Na_2CO_3 (887 mg, 8.4 mmol); ethyl bromoacetate (0.93 mL, 8.4 mmol). Crude yield: yellow oil (536 mg, 0.68 mmol, 81%). Yield after silica column chromatography: white solid (155 mg, 0.20 mmol, 24%). ^{1}H NMR (300 MHz, $CDCl_3$) δ 6.68–6.57 (m, 12H), 5.25 (q, ^3J = 7.2 Hz, 1H), 4.91 (d, ^2J = 13.5 Hz, 1H), 4.83 (d, ^2J = 13.7 Hz, 2H), 4.76–4.72 (m, 8H), 4.22 (q, ^3J = 7.2 Hz, 4H), 4.21 (q, ^3J = 7.2 Hz, 4H), 3.23 (d, ^2J = 13.7 Hz, 3H), 1.54 (d, ^3J = 7.2 Hz, 3H), 1.30 (t, ^3J = 7.2 Hz, 6H), 1.29 (t, ^3J = 7.2 Hz, 6H). ^{13}C NMR (75 MHz, $CDCl_3$) δ 170.19 (q), 170.07 (q), 155.86 (q), 155.53 (q), 139.57 (q), 134.85 (q), 134.56 (q), 134.23 (q), 128.49 (t), 128.43 (t), 125.03 (t), 122.95 (t), 122.82 (t), 71.52 (s), 71.31 (s), 60.54 (s), 60.48 (s), 31.51 (s), 31.44 (s), 30.97 (t), 20.45 (p), 14.21 (p). HRMS (ESI, *m/z*): Calculated for $C_{45}H_{50}O_{12}H^+$ ($[M+H]^+$): 783.3375, Found: 783.3378.

*4.1.9.2. 25,26,27,28-Tetra[(ethoxycarbonyl)methoxy]-2-propylcalix[4]arene (**10b**).* Precursor and reagents: **9b** (228 mg, 0.49 mmol); Na_2CO_3 (518 mg, 4.9 mmol); ethyl bromoacetate (0.54 mL, 4.9 mmol). Crude yield: yellow oil (373 mg, 0.46 mmol, 94%). Yield after silica column chromatography: white solid (122 mg, 0.15 mmol, 31%). ^{1}H NMR (300 MHz, $CDCl_3$) δ 6.67–6.55 (m, 12H), 5.02 (t, ^3J = 7.7 Hz, 1H), 4.89 (d, ^2J = 13.5 Hz, 2H), 4.86 (d, ^2J = 13.7 Hz, 1H), 4.85–4.68 (m, 8H), 4.23 (q, ^3J = 7.2 Hz, 4H), 4.20 (q,

^3J = 7.2 Hz, 4H), 3.24 (d, ^2J = 13.7 Hz, 1H), 3.22 (d, ^2J = 13.5 Hz, 2H), 1.88 (q, ^3J = 7.3 Hz, 2H), 1.48 (sext, ^3J = 7.3 Hz, 2H), 1.30 (t, ^3J = 7.2 Hz, 6H), 1.28 (t, ^3J = 7.2 Hz, 6H), 0.98 (t, ^3J = 7.3 Hz, 3H). ^{13}C NMR (75 MHz, $CDCl_3$) δ 170.24 (q), 169.97 (q), 155.93 (q), 155.73 (q), 138.22 (q), 134.75 (q), 134.61 (q), 134.50 (q), 128.48 (t), 128.43 (t), 128.31 (t), 125.29 (t), 122.94 (t), 122.77 (t), 71.50 (s), 71.15 (s), 60.49 (s), 60.44 (s), 36.63 (s), 36.39 (t), 31.69 (s), 31.39 (s), 21.47 (s), 14.48 (p), 14.24 (p), 14.19 (p). HRMS (ESI, *m/z*): Calculated for $C_{47}H_{54}O_{12}H^+$ ($[M+H]^+$): 811.3688, Found: 811.3675.

*4.1.9.3. 25,26,27,28-Tetra[(ethoxycarbonyl)methoxy]-2-pentylcalix[4]arene (**10c**).* Precursor and reagents: **9c** (500 mg, 1.01 mmol); Na_2CO_3 (1.07 g, 10.1 mmol); ethyl bromoacetate (1.12 mL, 10.1 mmol). Crude yield: yellow oil (472 mg, 0.56 mmol, 56%). Yield after silica column chromatography: white solid (138 mg, 0.16 mmol, 16%). ^{1}H NMR (300 MHz, $CDCl_3$) δ 6.70–6.55 (m, 12H), 4.99 (t, ^3J = 7.7 Hz, 1H), 4.90 (d, ^2J = 13.5 Hz, 2H), 4.85 (d, ^2J = 13.8 Hz, 1H), 4.85–4.68 (m, 8H), 4.23 (q, ^3J = 7.2 Hz, 4H), 4.19 (q, ^3J = 7.2 Hz, 4H), 3.24 (d, ^2J = 13.8 Hz, 1H), 3.22 (d, ^2J = 13.5 Hz, 2H), 1.88 (q, ^3J = 7.3 Hz, 2H), 1.51–1.38 (m, 2H), 1.38–1.26 (m, 4H), 1.30 (t, ^3J = 7.2 Hz, 6H), 1.28 (t, ^3J = 7.2 Hz, 6H), 0.88 (t, ^3J = 7.1 Hz, 3H). ^{13}C NMR (75 MHz, $CDCl_3$) δ 170.27 (q), 169.98 (q), 155.96 (q), 155.73 (q), 138.20 (q), 134.72 (q), 134.63 (q), 134.54 (q), 128.56 (t), 128.48 (t), 128.43 (t), 128.29 (t), 125.29 (t), 122.95 (t), 122.77 (t), 71.52 (s), 71.14 (s), 60.50 (s), 60.45 (s), 36.66 (t), 34.33 (s), 32.29 (s), 31.69 (s), 31.39 (s), 28.04 (s), 22.63 (s), 14.24 (p), 14.20 (p), 14.10 (p). HRMS (ESI, *m/z*): Calculated for $C_{49}H_{58}O_{12}Na^+$ ($[M+Na]^+$): 861.3820, Found: 861.3856.

*4.1.9.4. 25,26,27,28-Tetra[(ethoxycarbonyl)methoxy]-2-(prop-2′-yn-1′-yl)calix[4]arene (**10d**).* Precursor, solvents and reagents: **9d** (660 mg, ca. 1.4 mmol of crude **9d** obtained after deprotection of pure **8d**); anhydrous acetonitrile (25 mL); Na_2CO_3 (1.45 g, 13.7 mmol); ethyl bromoacetate (1.52 mL, 13.7 mmol). A slightly different workup was employed: after cooling down to room temperature, salts were removed by filtration, the filtrate concentrated *in vacuo*, and the residue was taken up in dichloromethane (100 mL) and water (100 mL). Layers were separated, and the water layer was washed with dichloromethane (2 × 50 mL). The combined organic extracts were dried over $MgSO_4$, filtered, evaporated *in vacuo*, and purified by silica column chromatography using a gradient of 30–60% of ethyl acetate in heptanes to obtain the pure target compound as a pale yellow glassy solid (401 mg, 0.50 mmol, 36%). ^{1}H NMR (300 MHz, $CDCl_3$) δ 6.70–6.58 (m, 12H), 5.36 (t, ^3J = 7.9 Hz, 1H), 4.95–4.72 (m, 11H), 4.25 (q, ^3J = 7.1 Hz, 4H), 4.20 (q, ^3J = 7.1 Hz, 4H), 3.25 (d, ^2J = 13.7 Hz, 1H), 3.23 (d, ^2J = 13.7 Hz, 2H), 2.82 (dd, ^3J = 7.9 Hz, ^4J = 2.6 Hz, 2H), 1.93 (t, ^4J = 2.6 Hz, 1H), 1.30 (t, ^3J = 7.1 Hz, 6H), 1.29 (t, ^3J = 7.1 Hz, 6H). ^{13}C NMR (75 MHz, $CDCl_3$) δ 170.20 (q), 170.05 (q), 155.93 (q), 155.79 (q), 136.66 (q), 134.65 (q), 134.64 (q), 134.59 (q), 128.98 (t), 128.55 (t), 128.41 (t), 124.88 (t), 122.98 (t), 122.84 (t), 83.60 (q), 71.73 (s), 71.26 (s), 69.72 (t), 60.56 (s), 60.50 (s), 36.04 (t), 31.64 (s), 31.38 (s), 23.67 (s), 14.24 (p), 14.19 (p). HRMS (ESI, *m/z*): Calculated for $C_{47}H_{50}O_{12}H^+$ ($[M+H]^+$): 807.3381, Found: 807.3388.

*4.1.10. General procedure for preparation of 25,26,27,28-tetrakis-N-(N,N-dimethyl-2-aminoethyl)carbamoylmethoxy-2-alkylcalix[4]arenes (**11a**–**d**)*

A solution of 25,26,27,28-tetra[(ethoxycarbonyl)methoxy]-2-alk(yn)ylcalix[4]arene **10a**–**d** (0.22–0.60 mmol) in *N,N*-dimethylethylenediamine (10 mL) was stirred at 50 °C for 48 h. The excess of *N,N*-dimethylethylenediamine was evaporated under reduced pressure and the resulting crystals were triturated twice with diethyl ether (first 10 mL, then 5 mL) and dried *in vacuo*. The crude product was then dissolved in 0.2 M aq. HCl, and purified by preparative HPLC on system A (see general methods). Fractions containing the product were pooled, evaporated at the rotary evaporator to remove the acetonitrile, and lyophilized to yield the TFA-salt of the pure product. To obtain the free tetra-amine, the salt was taken up in saturated aq. $NaHCO_3$ (30 mL) and extracted with dichloromethane (2 × 30 mL). The combined organic extracts were dried on $MgSO_4$, filtered, and evaporated *in vacuo*.

*4.1.10.1. 25,26,27,28-Tetrakis-N-(N,N-dimethyl-2-aminoethyl)carbamoylmethoxy-2-methylcalix[4]arene (**11a**).* Precursor: **10a** (176 mg, 224 μmol). Crude yield: off-white solid (170 mg, 179 μmol, 80%). Preparative HPLC on system A (see general methods): t_R (product) = 8.3–10.8 min (broad peak). Yield after preparative HPLC (TFA-salt): white solid (107 mg, 76 μmol, 34%). Yield after extraction (free tetra-amine): white solid (53 mg, 56 μmol, 25%). ^{1}H NMR (300 MHz, $CDCl_3$) δ 7.75 (bs, 2H), 7.61 (bs, 2H), 6.70–6.50 (m, 12H), 4.99 (q, ^3J = 7.2 Hz, 1H), 4.63 (d, ^3J = 14.1 Hz, 2H), 4.53–4.32 (m, 9H), 3.53–3.35 (m, 8H), 3.27 (d, ^2J = 14.1 Hz, 2H), 3.23 (d, ^2J = 12.8 Hz, 1H), 2.50–2.41 (m, 8H), 2.20 (bs, 24H), 1.49 (d, ^3J = 7.2 Hz, 3H). ^{13}C NMR (75 MHz, $CDCl_3$) δ = 169.55 (q), 169.53 (q), 155.75 (q), 155.66 (q), 139.48 (q), 134.43 (q), 134.15 (q), 133.83 (q), 128.88 (t), 128.82 (t), 128.76 (t), 125.37 (t), 123.29 (t), 123.22 (t), 74.36 (s), 74.09 (s), 58.15 (s), 58.13 (s), 45.36 (p), 45.34 (p), 37.14 (s), 37.09 (s), 31.45 (t), 31.21 (s), 31.09 (s), 20.31 (p). HRMS (ESI, *m/z*): Calculated for $C_{53}H_{74}N_8O_8H^+$ ($[M+H]^+$): 951.5702, Found: 951.5727.

*4.1.10.2. 25,26,27,28-Tetrakis-N-(N,N-dimethyl-2-aminoethyl)carbamoylmethoxy-2-propylcalix[4]arene (**11b**).* Precursor: **10b** (486 mg, 599 μmol). Crude yield: off-white solid (584 mg, 596 μmol, 99%). Preparative HPLC on system A: t_R (product) = 10.8–12.3 min. Yield after preparative HPLC (TFA-salt): white solid (343 mg, 239 μmol, 40%). Yield after extraction (free tetra-amine): white solid (158 mg, 161 μmol, 27%). ^{1}H NMR (300 MHz, $CDCl_3$) δ 7.77 (bs, 2H), 7.64 (bs, 2H), 7.71–6.50 (m, 12H), 4.88 (t, ^3J = 7.7 Hz, 1H), 4.64 (d, ^2J = 14.1 Hz, 2H), 4.57–4.32 (m, 9H), 3.52–3.36 (m, 8H), 3.28 (d, ^2J = 14.1 Hz, 2H), 3.22 (d, ^2J = 14.1 Hz, 1H), 2.50–2.41 (m, 8H), 2.21 (s, 12H), 2.20 (s, 12H), 1.91–1.77 (m, 2H), 1.46 (sext, ^3J = 7.2 Hz, 2H), 0.97 (t, ^3J = 7.2 Hz, 3H). ^{13}C NMR (75 MHz, $CDCl_3$) δ = 169.55 (q), 169.52 (q), 155.95 (q), 155.62 (q), 138.27 (q), 134.51 (q), 133.95 (q), 133.80 (q), 128.89 (t), 128.79 (t), 128.68 (t), 125.74 (t), 123.19 (t), 74.22 (s), 74.01 (s), 58.13 (s), 45.33 (p), 37.12 (s), 37.06 (s), 36.90 (t), 36.45 (s), 31.33 (s), 31.15 (s), 21.60 (s), 14.46 (p). HRMS (ESI, *m/z*): Calculated for $C_{55}H_{78}N_8O_8H^+$ ($[M+H]^+$): 979.6015, Found: 979.6026.

*4.1.10.3. 25,26,27,28-Tetrakis-N-(N,N-dimethyl-2-aminoethyl)carbamoylmethoxy-2-pentylcalix[4]arene (**11c**).* Precursor: **10c** (268 mg, 319 μmol). Crude yield: off-white solid (313 mg, 311 μmol, 97%). Preparative HPLC on system A: t_R (product) = 12.8–14.0 min. Yield after preparative HPLC (TFA-salt): white solid (177 mg, 121 μmol, 38%). Yield after extraction (free tetra-amine): white solid (110 mg, 109 μmol, 34%). ^{1}H NMR (300 MHz, $CDCl_3$) δ 7.77 (bs, 2H), 7.63 (bs, 2H), 6.70–6.48 (m, 12H), 4.87 (t, ^3J = 7.5 Hz, 1H), 4.65 (d, ^2J = 14.1 Hz, 2H), 4.56–4.30 (m, 9H), 3.52–3.37 (m, 8H), 3.28 (d, ^2J = 14.1 Hz, 2H), 3.22 (d, ^2J = 14.1 Hz, 1H), 2.52–2.40 (m, 8H), 2.22 (s, 12H), 2.21 (s, 12H), 1.91–1.77 (m, 2H), 1.51–1.36 (m, 2H), 1.36–1.23 (m, 4H), 0.88 (t, ^3J = 7.1 Hz, 3H). ^{13}C NMR (75 MHz, $CDCl_3$) δ 169.55 (q), 169.50 (q), 155.97 (q), 155.61 (q), 138.30 (q), 134.51 (q), 133.94 (q), 133.80 (q), 128.88 (t), 128.79 (t), 128.68 (t), 125.72 (t), 123.21 (t), 123.18 (t), 74.24 (s), 74.00 (s), 58.14 (s), 45.33 (p), 45.31 (p), 37.24 (t), 37.14 (s), 37.05 (s), 34.26 (s), 32.30 (s), 31.34 (s), 31.14 (s), 28.35 (s), 22.73 (s), 14.15 (p). HRMS (ESI, *m/z*): Calculated for $C_{57}H_{82}N_8O_8H^+$ ($[M+H]^+$): 1007.6328, Found: 1007.6350.

*4.1.10.4. 25,26,27,28-Tetrakis-N-(N,N-dimethyl-2-aminoethyl) carbamoylmethoxy-2-(prop-2′-yn-1′-yl)calix[4]arene (**11d**).* Precursor: **10d** (351 mg, 435 μmol). Instead of 50 °C for 48 h, the precursor was treated with *N,N*-dimethylethylenediamine (7.5 mL) at room temperature for 5 days. Crude yield: off-white solid (369 mg, 378 μmol, 87%). According to ^{1}H NMR, purity of this material was >90%. Part of the material (ca. 200 mg) was purified by preparative HPLC on system A: t_R (product) = 8.0–10.5 min. Yield after preparative HPLC (TFA-salt): pale yellow solid (170 mg, 119 μmol, 58%). Yield after extraction (free tetra-amine): white solid (68 mg, 70 μmol, 34%). ^{1}H NMR (300 MHz, $CDCl_3$) δ 7.86 (bs, 2H), 7.64 (bs, 2H), 6.70–6.51 (m, 12H), 5.29 (t, ^3J = 7.6 Hz, 1H), 4.75 (d, ^2J = 14.3 Hz, 2H), 4.52 (d, ^2J = 14.2 Hz, 3H), 4.36 (d, ^2J = 14.3 Hz, 6H), 3.58–3.38 (m, 8H), 3.31 (d, ^2J = 14.3 Hz, 2H), 3.22 (d, ^2J = 13.9 Hz, 1H), 2.73 (dd, ^3J = 7.8 Hz, ^4J = 2.4 Hz, 2H), 2.55–2.46 (m, 8H), 2.23 (s, 12H), 2.22 (s, 12H), 1.96 (t, ^4J = 2.4 Hz, 1H). ^{13}C NMR (75 MHz, $CDCl_3$) δ 169.60 (q), 169.53 (q), 156.07 (q), 155.75 (q), 136.84 (q), 134.54 (q), 133.85 (q), 133.81 (q), 129.35 (t), 128.89 (t), 128.84 (t), 125.51 (t), 123.27 (t), 123.23 (t), 83.19 (q), 74.37 (s), 74.13 (s), 70.05 (t), 58.12 (s), 58.08 (s), 45.31 (p), 37.09 (s), 37.06 (s), 36.45 (t), 31.41 (s), 31.03 (s), 23.56 (s). HRMS (ESI, *m/z*): Calculated for $C_{55}H_{74}N_8O_8H^+$ ($[M+H]^+$): 975.5708, Found: 975.5723.

*4.1.11. 25,26,27,28-Tetrakis-N-(N,N-dimethyl-2-aminoethyl) carbamoylmethoxy-2-{[1-(2-fluoroethyl)-1H-[1,2,3]triazo-4-yl] methyl}calix[4]arene (**13**)*

To a stirred solution of $CuSO_4 \times 5H_2O$ (67 mg, 268 μmol) and L-ascorbic acid (92 mg, 522 μmol) in water (3 mL) under an N_2 atmosphere was added a solution of crude **11d** (169 mg, 173 μmol) in *N,N*-dimethylformamide (2.5 mL) and 2-fluoroethylazide **5** (212 μmol; 3.6 mL of a 0.0588 M solution in *N,N*-dimethylformamide freshly prepared following published procedures [25]). The mixture was stirred at room temperature overnight, and then evaporated to dryness. The residue was treated with dichloromethane (15 mL) and aqueous Na_2CO_3 (15 mL). The layers were separated and the aqueous layer was extracted again with dichloromethane (2 × 15 mL). The combined organic layers were dried over $MgSO_4$, filtered, and evaporated *in vacuo* to yield the target compound (133 mg, 125 μmol, 72%). The crude material was taken up in a mixture of acetonitrile and water (ca. 2.5 mL) and purified by preparative HPLC on system A. Fractions containing the product (broad peak; t_R = 7.0–9.5 min) were pooled, partly evaporated at the rotary evaporator to remove the acetonitrile, and lyophilized to obtain the TFA-salt of **13** as a white solid (116 mg, 76 μmol, 44%). The solid was taken up in dichloromethane (30 mL) and thoroughly extracted with saturated aqueous $NaHCO_3$ (30 mL). The layers were separated and the aqueous layer was again extracted with dichloromethane (30 mL). The combined organic extracts were dried over $MgSO_4$, filtered, and evaporated to yield target compound **13** as the free tetra-amine. Yield: 48 mg (45 μmol, 26%) of a white solid. ^{1}H NMR (600 MHz, $CDCl_3$) δ 7.88 (bs, 2H), 7.78 (bs, 2H), 7.67 (s, 1H), 6.70–6.52 (m, 12H), 5.51 (t, ^3J = 8.0 Hz, 1H), 4.77 (dt, $^2J_{HF}$ = 46.8 Hz, $^3J_{HH}$ = 4.6 Hz, 2H), 4.64–4.37 (m, 11H), 4.24–4.13 (m, 2H), 3.51–3.38 (m, 8H), 3.32 (d, ^3J = 8.2 Hz, 2H), 3.26 (d, ^2J = 14.3 Hz, 2H), 3.23 (d, ^2J = 14.1 Hz, 1H), 2.53–2.40 (m, 8H), 2.23 (s, 24H). ^{13}C NMR (75 MHz, $CDCl_3$) δ 169.60 (q), 169.56 (q), 155.95 (q), 155.74 (q), 146.81 (q), 137.16 (q), 134.45 (q), 133.90 (q), 129.03 (t), 128.96 (t), 128.76 (t), 125.89 (t), 123.27 (t), 123.21 (t), 81.55 (s, doublet, $^1J_{CF}$ = 171 Hz), 74.13 (s), 73.95 (s), 58.16 (s), 58.00 (s), 50.43 (s, doublet, $^2J_{CF}$ = 21 Hz), 45.34 (p), 45.23 (p), 37.05 (s), 36.97 (s), 36.33 (t), 31.31 (s), 31.09 (s), 30.18 (s). HRMS (ESI, *m/z*): Calculated for $C_{57}H_{78}FN_{11}O_8H^+$ ($[M+H]^+$): 1064.6097, Found: 1064.6121.

*4.1.12. 1,1′-(((Oxybis(methylene))bis(oxy))bis(ethane-2,1-diyl)) bis(4-(25,26,27,28-(tetra-N-(N,N-dimethyl-2-aminoethyl) carbamoylmethoxy)calix[4]arene-2-yl)-1H-1,2,3-triazole) (**14**)*

Crude **11d** (100 mg, 102 μmol) was dissolved in *N,N*-dimethylformamide (2.4 mL) by slightly warming with a heat gun. Under N_2 atmosphere and continued stirring were added solutions of $CuSO_4 \times 5H_2O$ (38 mg, 152 μmol in 1 mL of water) and L-ascorbic acid (60 mg, 303 μmol in 1 mL of water), followed by a freshly prepared solution of 1,11-diazido-3,6,9-trioxaundecane **12** (12.4 mg, 50.8 μmol in 1 mL of *N,N*-dimethylformamide), and the reaction mixture was stirred at 50 °C overnight. For isolation of the product, aliquots of the reaction mixture were 1:1 diluted with 2 M aq. HCl, and purified by preparative HPLC on system A. Fractions containing the product (peak; t_R = 16.0–17.5 min) were pooled, evaporated at the rotary evaporator to remove the acetonitrile, and lyophilized to yield the TFA-salt of the pure product as a white solid (75 mg, 24 μmol, 47%). The solid was taken up in dichloromethane (20 mL), and thoroughly extracted with 1 M aqueous NaOH (20 mL). Layers were separated, and the aqueous layer was again extracted with dichloromethane (3 × 20 mL). The combined organic layers were dried on $MgSO_4$, filtered, and evaporated *in vacuo* to yield target compound **14** as the free tetra-amine. Yield: 44 mg (20 μmol, 39%) of a white fluffy solid. ^{1}H NMR (600 MHz, $CDCl_3$) δ 7.89 (bs, 4H), 7.85 (bs, 4H), 7.55 (s, 2H), 6.65–6.51 (m, 24H), 5.42 (t, ^3J = 7.9 Hz, 2H), 4.55–4.39 (m, 22H), 4.22 (d, ^2J = 13.5 Hz, 4H), 3.81 (t, ^3J = 5.3 Hz, 4H), 3.52–3.36 (m, 24H), 3.29 (d, ^3J = 7.8 Hz, 4H), 3.23 (d, ^2J = 14.2 Hz, 2H), 3.22 (d, ^2J = 14.2 Hz, 4H), 2.47–2.35 (m, 16H), 2.21 (s, 24H), 2.19 (s, 24H). ^{13}C NMR (150 MHz, $CDCl_3$) δ 169.57 (q), 169.42 (q), 155.83 (q), 155.63 (q), 145.95 (q), 137.04 (q), 134.44 (q), 134.08 (q), 133.91 (q), 128.94 (t), 128.85 (t), 128.71 (t), 125.76 (t), 123.20 (t), 123.12 (t), 74.00 (s), 70.42 (s), 70.33 (s), 69.43 (s), 58.15 (s), 58.00 (s), 50.08 (s), 45.36 (p), 45.33 (p), 37.09 (s), 37.06 (s), 36.26 (t), 31.17 (s), 31.04 (s), 30.02 (s). HRMS (ESI, *m/z*): Calculated for $C_{118}H_{164}N_{22}O_{19}H_2^{2+}$ ($[M+2H]^{2+}$): 1097.6344, Found: 1097.6384.

4.2. Cell viability assay

MA148 cells, a human epithelial ovarian carcinoma cell line, were seeded in non-coated 96-well plates (Corning; Lowell, MA), whereas human umbilical vein derived EC (HUVEC) were seeded in a 96-well culture plate coated with 0.2% gelatin for 2 h at 20 °C (Sigma–Aldrich; St. Louis, MO). Both cell types were seeded at a concentration of 3000 cells per well and allowed to adhere for at least 3 h at 37 °C in 5% CO_2/95% air before treatments were initiated. The cells were then exposed to complete medium, with or without various concentrations of 0118 for 72 h or as indicated otherwise. Cell counting kit (CCK-8; Dojindo; Gaithersburg, MD) was used to assess cell viability rates relative to untreated cells, as described earlier [42]. All measurements were done in triplicate, and the experiments were done at least three times. The IC50 was determined as half the maximal inhibitory drug concentration for each cell line. HUVEC and MA148 cells were kindly provided by Prof. Dr. Ramakrishnan (University of Minnesota) [43] and propagated as described earlier [44].

4.3. Radiochemistry

4.3.1. General materials and methods

Radiosynthesis was performed on a custom-designed 'ModularLab' system. The individual modules, which make up this 'ModularLab' system are commercially available from Eckert & Ziegler Eurotope GmbH (Berlin, Germany). The core of the system is made up of two Peltier reactor modules (PRM), which allow temperature control from −40 °C to +150 °C. Both are equipped with

temperature and radioactivity sensors, magnetic stirrers, reactor cameras and pneumatic reactor lifts. The reactions were performed in 3 mL borosilicate glass V-vials from Alltech (Grace Discovery Sciences, Deerfield, IL) equipped with reactor heads from Eckert & Ziegler and EPDM flat seals. Connections for liquid transfer were from PTFE and FEP tubing. Solvents were evaporated employing a constant stream of argon regulated by a flow controller module. Radioactive exhaust vapors were condensed in a vacuum trap cooled with liquid nitrogen, and subsequently passed through an activated carbon filter. Liquid transfers were performed using either vacuum or a positive pressure of argon (1.5 bar), or both. The valve modules used for assembling the system were 3/2-way and 2/2-way solenoid valve modules (SMC-valves type LVM), a single stopcock module, and stopcock manifold modules for gas transfer and the final radiopharmaceutical formulation step. Semi-preparative HPLC purification was performed on a SymmetryPrep C18 column (100 Å, 7 μm, 7.8 × 300 mm, Waters Corporation, Milford, MA) integrated into an HPLC module equipped with an electrically driven 6-port-multi-channel valve, an Omron E3X-DA-S fluid sensor, a preparative sample loop, a radioactivity detector in series with a WellChrom fixed wavelength detector K-200 ($\lambda = 254$ nm; Knauer GmbH, Berlin, Germany), and two WellChrom HPLC pumps K120 (Knauer GmbH). The complete system was placed in a hot-cell, whereas the PLC (programmable logic controller), the cooling unit, the cold trap and the shielded vacuum pump were located in the service corridor behind the hot-cell. All processes were remotely controlled on a PC employing the dedicated Modular-Lab software interface from Eckert & Ziegler, which allows straightforward set-up of the interactive process panel, flexible programming, and provides GMP-compliant batch records including temperature, activity, and UV traces.

Analytical HPLC-analysis for monitoring reaction progress and composition of crude products and for quality control of the final tracer product was carried out on an Agilent 1100 Series system with a binary pump and a variable wavelength UV-detector (preset to 271 nm, which is λ_{max} of **6**) in series with a Gabi-Star radioactivity detector (Raytest GmbH, Straubenhardt, Germany). The samples (20 μL) were injected onto a Symmetry C18 column (100 Å, 5 μm, 3.9 × 150 mm, Waters Corporation, Milford, USA), which was eluted at 1 mL/min with a linear gradient of acetonitrile (B) in water (A), both containing 0.1% TFA. Three different gradients were used for analysis of the intermediate 2-[^{18}F]fluoroethylazide [^{18}F]**5** (Gradient I: 3 min at 50% B followed by a linear gradient to 75% B in 7 min, a linear gradient to 95% B in 1 min, and subsequent isocratic elution for 2 min) and for analysis of click reaction mixtures and formulated radiotracers [^{18}F]**6** (Gradient II: 3 min at 30% B, followed by a linear gradient to 40% B in 5 min, isocratic elution for 2 min, a linear gradient to 95% B in 1 min, then isocratic elution at 95%B, return to 30% B, and equilibrating for at least 5 min before injection of the next sample) and [^{18}F]**13** (Gradient III: 3 min at 27% B, followed by a linear gradient to 29.5% B in 10 min, isocratic elution for 2 min, a linear gradient to 95% B in 1 min, then isocratic elution at 95%B, return to 27% B, and equilibrating for at least 5 min before injection of the next sample), respectively. Retention times (t_R) for the starting materials, intermediates, reference compounds and radiotracers (the latter based on the radio-trace) were as follows: 2-azidoethyl-4-methylbenzenesulfonate **15** (Gradient I: 5.5 min, Gradient II: 12.4 min); [^{18}F]**5** (Gradient I: 2.9 min; Gradient II: 4.6 min; Gradient III: 5.2 min); click precursor **4** (Gradient II: 7.6 min); reference compound **6** (Gradient II: 6.9 min), radiotracer [^{18}F]**6** (Gradient II: 7.3 min); click precursor **11d** (Gradient III: 11.3 min); reference compound **13** (Gradient III: 8.7 min), radiotracer [^{18}F]**13** (Gradient III: 9.1 min). UV and radioactivity detectors were arranged in series, leading to a delay of about 0.4 min in the radio-trace.

Radioactivity of the [^{18}F]-charged QMA-cartridges, [^{18}F]-intermediates, and the final product was measured in a calibrated digital ionization chamber (model VIK-202, Veenstra Instruments, Joure, The Netherlands). Water was purified and de-ionized (18 MΩ cm) by means of a Milli-Q water filtration system (Millipore). The Sep-Pak® Plus Light C_8 cartridges for solid phase extraction were purchased from Waters (USA). The syringe filters (GD/X syringe filter, PTFE, 0.45 μm, with borosilicate prefilter) for filtration of the crude click reaction mixture were from Whatman (UK). Anhydrous acetonitrile and Kryptofix 222 were from Merck, tris[(1-benzyl-1*H*-1,2,3-triazol-4-yl)methyl]amine (TBTA) and (R)-(−)-(3,5-dioxa-4-phosphacyclohepta[2,1-a:3,4-a′]dinaphthalen-4-yl)dimethylamine (MonoPhos) from Sigma–Aldrich, and 4,7-diphenyl-1,10-phenanthroline disulfonic acid (BPDS) from Pfaltz & Bauer, Inc. (USA). Purity of all ligands was >96% (HPLC). All other reagents, catalysts, and solvents were obtained from Acros (Belgium) or Sigma–Aldrich and were used without further purification.

4.3.2. Radiosynthesis of 2-[^{18}F]fluoroethylazide [^{18}F]**5**

[^{18}F]F$^-$ was purchased from BV Cyclotron VU (Amsterdam, The Netherlands). It was produced by the ^{18}O(p,n)^{18}F nuclear reaction in an IBA 18/9 cyclotron and subsequently trapped on a QMA-cartridge (Waters Sep-Pak® Plus Light QMA; carbonate form) for shipment. After arrival at our facilities (about 1–2 half-lives after EOB), [^{18}F]F$^-$ was eluted from the anion exchange column into a 3 mL V-vial using 1 mL of acetonitrile/water (9/1, v/v), which contained Kryptofix 222 (13 mg, 34 μmol) and K_2CO_3 (2 mg, 14 μmol). The solution was dried under an argon flow (~70 mL/min) and reduced pressure at 70 °C for 5 min, 100 °C for 2 min, and 110 °C for 6 min (4 min lift-position 'up' and 2 min lift-position 'down'). To remove residual water, anhydrous acetonitrile (0.9 mL) was added, and the solution was dried again at 70 °C for 2 min and 110 °C for 3 min (2 min lift-position 'up' and 1 min lift-position 'down'). This co-evaporation cycle was repeated once.

After cooling to 40 °C, a solution of 2-azidoethyl-4-methylbenzenesulfonate **15** (5 μL; prepared according to published procedures [32,33] with minor modifications) in anhydrous acetonitrile (0.7 mL) was added to the K[^{18}F]F–K222 residue, allowed to react for 15 min at 80 °C, and the intermediate 2-[^{18}F]fluoroethylazide [^{18}F]**5** was co-distilled at 90 °C under a constant stream of argon (20 mL/min) into a 3 mL septum-capped V-vial, which was pre-cooled to −40 °C. After 10 min, the integrated radioactivity detectors in the reactors indicated that distillation was complete, and the radioactivity collected in the receiver vial was measured in a dose calibrator. Decay-corrected isolated radiochemical yield of 2-[^{18}F]fluoroethylazide was 53 ± 5% (n = 10). HPLC-analysis of the distillate indicated absence of precursor **15** in the UV-trace and a radiochemical purity of >99%. The volume of the 2-[^{18}F]fluoroethylazide distillate in acetonitrile in these experiments was about 300–400 μL.

4.3.3. Optimization of CuAAC conditions for reaction of [^{18}F]**5** with precursor **11d**

Stock solutions of precursor **11d** (1.46 mg, 1.5 μmol) were prepared in: A) 250 μL of DMSO (Table 2, entries 1, 2, 5, 6, 8, 9, 10, 13, and 14); B) 200 μL of DMSO (Table 2, entries 3, 4, 11, and 12); C) 50 μL of sodium phosphate buffer pH 6.0 and 200 μL of water (Table 2, entry 7).

Ligand stock solutions: TBTA and MonoPhos were dissolved in DMSO at a concentration of 16.5 mM (Table 2, entries 3, 4, 11 and 12), and BPDS was dissolved in water at the same concentration (Table 2, entry 2, 5, 10, and 13), or at 99.0 mM (Table 2, entry 8).

Catalyst stock solutions: Solutions of $CuSO_4 \times 5H_2O$ and sodium L-ascorbate were freshly prepared before each experiment.

$CuSO_4 \times 5H_2O$ was dissolved in water at the following concentrations: A) 10 mM (Table 2, entries 1, 3, 4, 9, 11, 12); B) 30 mM (Table 2, entries 2, 5, 10, 13); C) 60 mM (Table 2, entries 6, 7, 14); D) 180 mM (Table 2, entry 8). Sodium L-ascorbate stock solutions were as follows: A) 150 mM in 0.5 M sodium phosphate buffer pH 6.0 (Table 2, entries 1, 2, 3, 4, 9, 10, 11, 12); B) 150 mM in 0.5 M Tris/HCl-buffer pH 8.5 (Table 2, entries 5 and 13); C) 900 mM in 0.5 M sodium phosphate buffer pH 6.0 (Table 2, entries 6 and 14); C) 900 mM in 0.5 M Tris/HCl-buffer pH 8.5 (Table 2, entry 8); D) 900 mM in water (Table 2, entry 7).

Experimental procedure: When applicable, ligand stock solutions (50 μL) were first added to the solution of precursor **11d** in a 3 mL V-vial containing a magnetic stirring bar. Immediately before addition to the precursor solution, the catalyst mixture was prepared as follows: Aqueous $CuSO_4$-solutions, 150 μL (Table 2, entries 1, 3, 4, 6, 7, 9, 11, 12, and 14; concentration depending on experiment, see above) or 50 μL (Table 2, entries 2, 5, 8, 10, 13; concentration depending on experiment, see above) were mixed with aqueous Na-ascorbate solutions (100 μL, concentration and buffer depending on experiment, see above), and then half of the total volume was added to the corresponding precursor solution. A solution of 2-[^{18}F]fluoroethylazide in acetonitrile (150 μL, 50–150 MBq) was added, and the solution was thoroughly mixed by pipetting up and down. The reaction vial was then sealed with a septum screw cap, and the mixture was incubated at the indicated temperature (23 °C or 80 °C), while stirring with a magnetic stirring bar. After 15 min and 30 min, samples were retrieved using a syringe, and frozen in liquid nitrogen. Immediately before HPLC analysis, samples were thawed by diluting to an appropriate activity concentration with water containing 0.1% TFA, and directly injected. Analytical yield (conversion) was calculated based on the peak areas of unreacted 2-[^{18}F]fluoroethylazide and click product [^{18}F]**13** in the radio-trace.

4.3.4. Radiosynthesis, purification, and formulation of [^{18}F]**6** and [^{18}F]**13**

The intermediate 2-[^{18}F]fluoroethylazide [^{18}F]**5** – prepared as described in Section 4.3.2 – was co-distilled at 90 °C under a constant stream of argon (20 mL/min) into a 3 mL septum-capped V-vial pre-cooled to −40 °C, which contained a solution of precursor **11d** (2.9 mg, 3 μmol) or **4** (2.6 mg, 3 μmol) in DMSO (500 μL). In the meantime, stock solutions of 60 mM $CuSO_4 \times 5H_2O$ in water and 900 mM sodium L-ascorbate in 0.5 M sodium phosphate buffer pH 6.0 were prepared. When co-distillation of [^{18}F]**5** was complete (ca. 10 min), the collector vial was quickly warmed up to room temperature, and 250 μL of the aqueous catalyst mixture (prepared immediately before addition to the reaction vessel by mixing 300 μL of the $CuSO_4 \times 5H_2O$-stock solution with 200 μL of the Na-ascorbate stock solution) was manually added via a syringe, which corresponds to 3 equiv. of $CuSO_4$ (9 μmol) and 30 equiv. of ascorbate (90 μmol) in the final reaction mixture. Following reaction at 80 °C for 15 min, the reaction mixture was diluted with water acidified with 0.1% TFA (1.5 mL) and loaded onto the C18 semi-preparative HPLC-column pre-conditioned with the initial eluent mixture (for [^{18}F]**6**: 30% acetonitrile in water – both eluents containing 0.1% TFA; for [^{18}F]**13**: 27% acetonitrile in water – both eluents containing 0.1% TFA) via a preparative sample loop. The flow was increased stepwise from 2 mL/min to 7 mL/min within 1 min, and elution with the initial eluent mixture was continued for 3.5 min, followed by a linear gradient (for [^{18}F]**6**: 30%–40% in 5 min followed by isocratic elution for 5 min; for [^{18}F]**13**: 27%–29.5% in 10 min). Retention time for [^{18}F]**6** and [^{18}F]**13** on these systems was about 9 min. The product fraction (total volume ca. 1.5–2 mL) was diverted into a septum-capped bottle containing water (35 mL). The purified radiotracers were trapped on a C_8 Sep-Pak® cartridge, rinsed with water (9 mL), eluted with ethanol (1 mL) into a 3 mL V-vial, evaporated to dryness at 80 °C under a stream of argon, and redissolved in DMSO to the desired target concentration for subsequent *in vitro* and *in vivo* studies.

4.4. In vitro characterization of radiotracers

4.4.1. Distribution coefficient Log $D_{7.4}$ in 1-octanol/PBS pH 7.4

Log $D_{7.4}$ values were measured using the shake flask method. To 1-octanol (0.5 mL) and PBS pH 7.4 (0.5 mL), which had been presaturated with each other, was added 1 μL of the final purified radiotracer stock solution in DMSO (ca. 1 MBq, radiochemical purity as determined by analytical HPLC was >98%), and the solvents were thoroughly mixed in an eppendorf mixer for 30 min (in addition, the tubes were manually mixed in 5–10 min intervals using a vortex). Following phase separation by centrifugation in an eppendorf centrifuge at 16,100 rcf for 5 min, aliquots of both phases (3 × 25 μL for each phase) were counted in a γ-counter (Wizard 1480; PerkinElmer). Log *D* was calculated as log (cpm in octanol/cpm in PBS).

4.4.2. Radiotracer stability in PBS pH 7.4 and in mouse serum

The radiotracers were incubated at 37 °C under gentle agitation (350 rpm) in either PBS pH 7.4 or mouse serum (Balb/C mouse serum, purchased from Innovative Research, and filtered through a 0.45 μm PTFE syringe filter before use) at activity concentrations of 10–15 MBq/mL, and 25–50 MBq/mL, respectively. Maximum DMSO concentration in the incubation mixtures (due to addition of the tracer stock solution in DMSO) was below 2%. For the PBS-incubation, aliquots were removed after 0, 1, 2, and 3 h, and directly analyzed by radio-HPLC. For the serum samples, aliquots (150–250 μL) were retrieved (same time points), thoroughly mixed with an equal volume of ice-cold acetonitrile (−20 °C), and proteins separated by centrifugation in an Eppendorf centrifuge (16,100 rcf, 5 min). An aliquot of the supernatant was removed for radio-HPLC, and another aliquot (50 μL) for measuring of radioactivity in the supernatant. To quantify probe binding to serum proteins, the remaining supernatant was discarded, and radioactivity of the pellet and supernatant-aliquot determined in the gamma counter. Importantly, before injection into the HPLC, supernatants were first 10-fold diluted with eluent A (0.1% TFA in water). To eliminate any effects due to sample processing, stability values (% intact radiotracer) were reported relative to the control sample ($t = 0$), for which the amount of intact probe was set to 100%.

4.5. Animal studies

Mice were housed and handled according to institutional guidelines complying with European legislation and the Dutch national law "Wet op de Dierproeven" (Staatsblad 1985, 336). Approval of the local IACUC was obtained prior to the commencement of the studies. Female nude BALB/c mice (19–24 g body weight; Charles River Laboratories, USA) were inoculated subcutaneously with 3×10^6 MDA-MB-231-LITG cells in 100 μL of sterile phosphate-buffered saline and were used when the tumors had reached a size of 70–350 mm^3 (typically after 17–23 days); tumor weights as determined after dissection were 0.141 ± 0.077 g ($n = 12$). Animals were kept in a temperature-controlled environment with a 12-h light/12-h dark cycle. They received a standard diet (Sniff R/M-H, Sniff Spezialdiäten GmbH, Soest, The Netherlands) and acidified water *ad libitum*.

Four groups of mice ($n = 3$–4) were intravenously injected with radiotracers [^{18}F]**6** (0.2–0.3 MBq, ca. 60 ng of **6** for the low-dose biodistribution; ~3.5 MBq, ca. 1 μg of **6** for the blood kinetics) and [^{18}F]**13** (0.3–0.4 MBq, ca. 100 ng of **13** for the low-dose

biodistribution; ~8.5 MBq, ca. 1 μg of **13** for the blood kinetics), administered as solutions in 10 mM sodium phosphate-buffered 0.9% saline (pH 5.5) containing 10% vol. DMSO. To assess blood clearance, blood samples (20–30 μL) were drawn from the vena saphena at 2–5–10–30–60–120 min post radiotracer injection. After 3 h, mice were euthanized by cervical dislocation, blood was obtained by cardiac puncture, and selected tissues and organs were harvested, blotted dry and weighed. Phosphate-buffered saline (1 mL) was then added to the samples, and sample radioactivity was measured in a γ-counter (Wizard 1480 from PerkinElmer; energy window 400–600 keV) along with standards to determine the percentage of injected dose per gram of tissue (%ID/g) and the percentage of injected dose per organ (%ID/organ). For blood, muscle, and bone, the uptake of tracer as %ID/organ was calculated from the %ID/g values assuming that these organs constitute 6, 41, and 11% of the body weight. The %ID/organ values for stomach, small and large intestines relate to organ including content. Data analysis was performed with GraphPad Prism version 6.04. All data are presented as mean %ID/g or %ID/organ ± one standard deviation (SD). *P*-values were calculated using a 2-tailed unpaired Student's *t*-test. Differences were considered statistically significant when the *P*-value was less than 0.05. For calculation of blood half-lives, blood clearance data was fitted using two-phase exponential decay functions ([^{18}F]**6**: $R^2 = 0.987$; [^{18}F]**13**: $R^2 = 0.998$).

For PET-CT imaging, mice were anesthetized using medical air containing 2–3% isoflurane (0.4 L/min), and anesthesia was maintained throughout the whole experimental procedure with medical air containing 1–2% isoflurane (0.4 L/min). Body temperature was stabilized by heating the animal bed via a continuous flow of warm air. After sedation, the tail vein was cannulated and radiotracers [^{18}F]**6** (12 MBq, 4.8 nmol) and [^{18}F]**13** (13 MBq, 3.7 nmol) were administered as solutions in 10 mM sodium phosphate-buffered 0.9% saline (pH 5.5) containing 10% vol. DMSO. Immediately after injection of the radiotracers, a 2 h whole body PET list-mode scan was acquired on a MOSAIC Animal PET scanner (Philips Medical Systems, Cleveland, OH) with an axial resolution of 2.2 mm, and a transmission scan using a Cs-137 external source was performed for attenuation correction. After the PET-scan, a whole-body CT scan with a resolution of 0.1 mm was acquired on a NanoSPECT-CT scanner (Bioscan Inc., Washington, DC). The animal positioning was kept constant during both scans. To enhance soft tissue contrast, the acquisition parameters were set to 45 kV peak tube voltage, 80 mm field of view, and 360 projections at 2000 ms per projection. After the scan, blood was retrieved by cardiac puncture, and animals were sacrificed by cervical dislocation and dissected. Selected tissues were counted in the γ-counter as described above. %ID/g and %ID/organ values were similar to the biodistribution results obtained for the two groups of mice employed for the blood clearance study (results not shown here). PET images for the timeframes of interest were reconstructed with a 3DRAMLA algorithm employing attenuation correction, and CT images with an Exact Cone Beam Filtered Back Projection (Logan filter) to a resolution of 0.1 mm × 0.1 mm × 0.1 mm. Co-registration of PET and CT images was performed with a Philips IMALYTICS Research Workstation (Version 3.0, Philips Research, Aachen, Germany) based on anatomical landmarks and a rigid registration algorithm. Volumes of interest (VOI) for analysis of tracer levels in muscle and tumor were defined by manual segmentation of the reconstructed CT images.

Conflict of interest

Co-authors A.W. Griffioen and K.H. Mayo have a financial interest in PepTx, a pharmaceutical company holding license on PTX compounds. T. Läppchen, R. Rossin, K. Donato, J. Lub, and H. Grüll are employees of Philips Electronics Nederland B.V.

Acknowledgments

We thank Mariëlle van Egmond for synthesis of tetramethoxycalix[4]arene **7**, and we thank Jeroen Pikkemaat, Jeroen P.W. van den Berg, and Hugo Knobel for technical support with NMR- and LC-MS analyses. Dr. Iris Verel, Caren van Kammen, Carlijn van Helvert, and Monique Berben are gratefully acknowledged for assistance in planning and executing of the *in vivo* studies. This work was financially supported by the Center for Translational Molecular Medicine – Mammary Carcinoma Molecular Imaging for Diagnosis and Therapeutics (CTMM-MAMMOTH), contract 2010249, project number 03O-201.

Appendix A. Supplementary data

Supplementary data related to this article can be found at http://dx.doi.org/10.1016/j.ejmech.2014.10.048. These data include MOL files and InChiKeys of the most important compounds described in this article.

References

[1] S. Chakrabarti, C.J. Barrow, R.K. Kanwar, V. Ramana, J.R. Kanwar, Current protein-based anti-angiogenic therapeutics, Mini Rev. Med. Chem. 14 (2014) 291–312.
[2] J. Folkman, Tumor angiogenesis: therapeutic implications, N. Engl. J. Med. 285 (1971) 1182–1186.
[3] M.S. O'Reilly, L. Holmgren, Y. Shing, C. Chen, R.A. Rosenthal, M. Moses, W.S. Lane, Y. Cao, E.H. Sage, J. Folkman, Angiostatin: a novel angiogenesis inhibitor that mediates the suppression of metastases by a Lewis lung carcinoma, Cell 79 (1994) 315–328.
[4] Y. Cao, R. Langer, A review of Judah Folkman's remarkable achievements in biomedicine, Proc. Natl. Acad. Sci. U. S. A. 105 (2008) 13203–13205.
[5] R.P. Dings, I. Nesmelova, A.W. Griffioen, K.H. Mayo, Discovery and development of anti-angiogenic peptides: a structural link, Angiogenesis 6 (2003) 83–91.
[6] A.W. Griffioen, D.W.J. van der Schaft, A.F. Barendsz-Janson, A. Cox, H.A.J.S. Boudier, H.F.P. Hillen, K.H. Mayo, Anginex, a designed peptide that inhibits angiogenesis, Biochem. J. 354 (2001) 233–242.
[7] R.P.M. Dings, M. Loren, H. Heun, E. McNiel, A.W. Griffioen, K.H. Mayo, R.J. Griffin, Scheduling of radiation with angiogenesis inhibitors anginex and avastin improves therapeutic outcome via vessel normalization, Clin. Cancer Res. 13 (2007) 3395–3402.
[8] D.W.J. van der Schaft, R.P.M. Dings, Q.G. de Lussanet, L.I. van Eijk, A.W. Nap, R.G.H. Beets-Tan, J.C.A.B.T. Steege, J. Wagstaff, K.H. Mayo, A.W. Griffioen, The designer antiangiogenic peptide anginex targets tumor endothelial cells and inhibits tumor growth in animal models, FASEB J. 16 (2002) 1991–1993.
[9] R.P.M. Dings, D.W.J. van der Schaft, B. Hargittai, J. Haseman, A.W. Griffioen, K.H. Mayo, Anti-tumor activity of the novel angiogenesis inhibitor anginex, Cancer Lett. 194 (2003) 55–66.
[10] A.E.M. Dirkx, M.G.A.O. Egbrink, K. Castermans, D.W.J. van der Schaft, V.L.J.L. Thijssen, R.P.M. Dings, L. Kwee, K.H. Mayo, J. Wagstaff, J.C.A.B.T. Steege, A.W. Griffioen, Anti-angiogenesis therapy can overcome endothelial cell anergy and promote leukocyte-endothelium interactions and infiltration in tumors, FASEB J. 20 (2006) 621–630.
[11] K.H. Mayo, R.P.M. Dings, C. Flader, I. Nesmelova, B. Hargittai, D.W.J. van der Schaft, L.I. van Eijk, D. Walek, J. Haseman, T.R. Hoye, A.W. Griffioen, Design of a partial peptide mimetic of anginex with antiangiogenic and anticancer activity, J. Biol. Chem. 278 (2003) 45746–45752.
[12] R.P.M. Dings, X.M. Chen, D.M.E.I. Hellebrekers, L.I. van Eijk, Y. Zhang, T.R. Hoye, A.W. Griffioen, K.H. Mayo, Design of nonpeptidic topomimetics of antiangiogenic proteins with antitumor activities, J. Natl. Cancer Inst. 98 (2006) 932–936.
[13] R.P.M. Dings, M.C. Miller, I. Nesmelova, L. Astorgues-Xerri, N. Kumar, M. Serova, X.M. Chen, E. Raymond, T.R. Hoye, K.H. Mayo, Antitumor agent calixarene 0118 targets human galectin-1 as an allosteric inhibitor of carbohydrate binding, J. Med. Chem. 55 (2012) 5121–5129.
[14] V.L.J.L. Thijssen, R. Postel, R.J.M.G.E. Brandwijk, R.P.M. Dings, I. Nesmelova, S. Satijn, N. Verhofstad, Y. Nakabeppu, L.G. Baum, J. Bakkers, K.H. Mayo, F. Poirier, A.W. Griffioen, Galectin-1 is essential in tumor angiogenesis and is a target for antiangiogenesis therapy, Proc. Natl. Acad. Sci. U. S. A. 103 (2006) 15975–15980.
[15] H. Leffler, U.J. Nilsson, Low-molecular weight inhibitors of galectins, in: A.A. Klyososv, P.G. Traber (Eds.), Galectins and Disease – Implications for Targeted Therapeutics, ACS Symposium Series, vol. 1115, American Chemical Society, Washington DC, 2012, pp. 47–59.

[16] P.M. Collins, C.T. Oberg, H. Leffler, U.J. Nilsson, H. Blanchard, Taloside inhibitors of galectin-1 and galectin-3, Chem. Biol. Drug Des. 79 (2012) 339–346.
[17] L. Astorgues-Xerri, M.E. Riveiro, A. Tijeras-Raballand, M. Serova, C. Neuzillet, S. Albert, E. Raymond, S. Faivre, Unraveling galectin-1 as a novel therapeutic target for cancer, Cancer Treat. Rev. 40 (2014) 307–319.
[18] L. Astorgues-Xerri, M.E. Riveiro, A. Tijeras-Raballand, M. Serova, G.A. Rabinovich, I. Bieche, M. Vidaud, A. de Gramont, M. Martinet, E. Cvitkovic, S. Faivre, E. Raymond, OTX008, a selective small-molecule inhibitor of galectin-1, downregulates cancer cell proliferation, invasion and tumour angiogenesis, Eur. J. Cancer 50 (2014) 2463–2477.
[19] R.P.M. Dings, J.I. Levine, S.G. Brown, L. Astorgues-Xerri, J.R. MacDonald, T.R. Hoye, E. Raymond, K.H. Mayo, Polycationic calixarene PTX013, a potent cytotoxic agent against tumors and drug resistant cancer, Invest. New Drugs 31 (2013) 1142–1150.
[20] K. Iwamoto, K. Araki, S. Shinkai, Conformations and structures of tetra-*O*-alkyl-*p*-*tert*-butylcalix[4]arenes. How is the conformation of calix[4]arenes immobilized? J. Org. Chem. 56 (1992) 4955–4962.
[21] H. Shimizu, K. Iwamoto, K. Fujimoto, S. Shinkai, Chromogenic calix[4]arene, Chem. Lett. 20 (1991) 2147–2150.
[22] J. Cooper, M. Drew, P. Beer, Alkali metal cation cooperative anion recognition by heteroditopic bis(calix[4]arene) rhenium(I) bipyridyl and ferrocene receptor molecules, J. Chem. Soc. Dalton Trans. 16 (2000) 2721–2728.
[23] C.M. Shu, W.S. Chung, S.H. Wu, Z.C. Ho, L.G. Lin, Synthesis of calix[4]arenes with four different "lower rim" substituents, J. Org. Chem. 64 (1999) 2673–2679.
[24] L.H. Bryant Jr., A.T. Yordanov, J.J. Linnoila, M.W. Brechbiel, J.A. Frank, First noncovalently bound calix[4]arene-Gd-III-albumin complex, Angew. Chem. Int. Ed. 39 (2000) 1641–1643.
[25] M. Glaser, E. Arstad, "Click labeling" with 2-[^{18}F]fluoroethylazide for positron emission tomography, Bioconjugate Chem. 18 (2007) 989–993.
[26] P.A. Scully, T.M. Hamilton, J.L. Bennett, Synthesis of 2-alkyl- and 2-carboxy-p-tert-butylcalix[4]arenes via the lithiation of tetramethoxy-p-tert-butylcalix[4]arene, Org. Lett. 3 (2001) 2741–2744.
[27] M.P. Hertel, A.C. Behrle, S.A. Williams, J.A.R. Schmidt, J.L. Fantini, Synthesis of amine, halide, and pyridinium terminated 2-alkyl-p-tert-butylcalix[4]arenes, Tetrahedron 65 (2009) 8657–8667.
[28] F. Arnaudneu, E.M. Collins, M. Deasy, G. Ferguson, S.J. Harris, B. Kaitner, A.J. Lough, M.A. Mckervey, E. Marques, B.L. Ruhl, M.J. Schwingweill, E.M. Seward, Synthesis, X-ray crystal-structures, and cation-binding properties of alkyl calixaryl esters and ketones, a new family of macrocyclic molecular receptors, J. Am. Chem. Soc. 111 (1989) 8681–8691.
[29] E.H. Ryu, Y. Zhao, Efficient synthesis of water-soluble calixarenes using click chemistry, Org. Lett. 7 (2005) 1035–1037.
[30] V.V. Rostovtsev, L.G. Green, V.V. Fokin, K.B. Sharpless, A stepwise Huisgen cycloaddition process: copper(I)-catalyzed regioselective "ligation" of azides and terminal alkynes, Angew. Chem. Int. Ed. 41 (2002) 2596–2599.
[31] S. Cecioni, R. Lalor, B. Blanchard, J.P. Praly, A. Imberty, S.E. Matthews, S. Vidal, Achieving high affinity towards a bacterial lectin through multivalent topological isomers of calix[4]arene glycoconjugates, Chem. Eur. J. 15 (2009) 13232–13240.
[32] Z.P. Demko, K.B. Sharpless, An intramolecular [2+3] cycloaddition route to fused 5-heterosubstituted tetrazoles, Org. Lett. 3 (2001) 4091–4094.
[33] D. Kobus, Y. Giesen, R. Ullrich, H. Backes, B. Neumaier, A fully automated two-step synthesis of an ^{18}F-labelled tyrosine kinase inhibitor for EGFR kinase activity imaging in tumors, Appl. Radiat. Isot. 67 (2009) 1977–1984.
[34] H.S. Gill, J.N. Tinianow, A. Ogasawara, J.E. Flores, A.N. Vanderbilt, H. Raab, J.M. Scheer, R. Vandlen, S.P. Williains, J. Marik, A modular platform for the rapid site-specific radiolabeling of proteins with F-18 exemplified by quantitative positron emission tomography of human epidermal growth factor receptor 2, J. Med. Chem. 52 (2009) 5816–5825.
[35] L. Iddon, J. Leyton, B. Indrevoll, M. Glaser, E.G. Robins, A.J.T. George, A. Cuthbertson, S.K. Luthra, E.O. Aboagye, Synthesis and in vitro evaluation of [^{18}F]fluoroethyl triazole labelled [Tyr^3]octreotate analogues using click chemistry, Bioorg. Med. Chem. Lett. 21 (2011) 3122–3127.
[36] W.G. Lewis, F.G. Magallon, V.V. Fokin, M.G. Finn, Discovery and characterization of catalysts for azide-alkyne cycloaddition by fluorescence quenching, J. Am. Chem. Soc. 126 (2004) 9152–9153.
[37] L.S. Campbell-Verduyn, L. Mirfeizi, R.A. Dierckx, P.H. Elsinga, B.L. Feringa, Phosphoramidite accelerated copper(I)-catalyzed [3+2] cycloadditions of azides and alkynes, Chem. Commun. (2009) 2139–2141.
[38] H.C. Kolb, M.G. Finn, K.B. Sharpless, Click chemistry: diverse chemical function from a few good reactions, Angew. Chem. Int. Ed. 40 (2001) 2004–2021.
[39] F.L. Zhang, J.P. Xue, J.W. Shao, L. Jia, Compilation of 222 drugs' plasma protein binding data and guidance for study designs, Drug Discov. Today 17 (2012) 475–485.
[40] R. Baynes, J.E. Riviere, Hepatic biotransformation and biliary excretion, in: Comparative Pharmacokinetics – Principles, Techniques, and Applications, Wiley-Blackwell, Oxford, 2011, pp. 113–141.
[41] C.D. Gutsche, B. Dhawan, J.A. Levine, K.H. No, L.J. Bauer, Calixarenes 9-Conformational isomers of the ethers and esters of calix[4]arenes, Tetrahedron 39 (1983) 409–426.
[42] R.P. Dings, M.M. Arroyo, N.A. Lockwood, L.I. van Eijk, J.R. Haseman, A.W. Griffioen, K.H. Mayo, Beta-sheet is the bioactive conformation of the anti-angiogenic anginex peptide, Biochem. J. 373 (2003) 281–288.
[43] R.P. Dings, Y. Yokoyama, S. Ramakrishnan, A.W. Griffioen, K.H. Mayo, The designed angiostatic peptide anginex synergistically improves chemotherapy and antiangiogenesis therapy with angiostatin, Cancer Res. 63 (2003) 382–385.
[44] R.P.M. Dings, B.W. Williams, C.W. Song, A.W. Griffioen, K.H. Mayo, R.J. Griffin, Anginex synergizes with radiation therapy to inhibit tumor growth by radiosensitizing endothelial cells, Int. J. Cancer 115 (2005) 312–319.